ARTICLE
Journal of Cellular Biochemistry 113:2920–2936 (2012)

Journal of Cellular Biochemistry

# A Novel Nuclear FGF Receptor-1 Partnership With Retinoid and Nur Receptors During Developmental Gene Programming of Embryonic Stem Cells

Yu-Wei Lee,[1] Christopher Terranova,[1] Barbara Birkaya,[1] Sridhar Narla,[1] Daniel Kehoe,[2] Abhirath Parikh,[2] Shuo Dong,[3] Andreas Ratzka,[4] Hella Brinkmann,[4] John M. Aletta,[5] Emmanuel S. Tzanakakis,[2,6] Ewa K. Stachowiak,[1,6] Peter Claus,[4*] and Michal K. Stachowiak[1,6**]

[1] *Molecular and Structural Neurobiology and Gene Therapy Program, Department of Pathology and Anatomical Sciences, State University of New York, Buffalo, New York 14214*

[2] *Department of Chemical and Biological Engineering, State University of New York, Buffalo, New York 14214*

[3] *Department of Medicine, Baylor College of Medicine, Houston, Texas 77030*

[4] *Institute of Neuroanatomy, Hannover Medical School, Carl-Neuberg-Str. 1, 30625 Hannover, Germany*

[5] *CH3 BioSystems, New York State Center of Excellence in Bioinformatics & Life Sciences, Buffalo, New York 14203*

[6] *Western New York Stem Cells Culture and Analysis Center, Buffalo, New York 14213*

## ABSTRACT

FGF Receptor-1 (FGFR1), a membrane-targeted protein, is also involved in independent direct nuclear signaling. We show that nuclear accumulation of FGFR1 is a common response to retinoic acid (RA) in pluripotent embryonic stem cells (ESC) and neural progenitors and is both necessary and sufficient for neuronal-like differentiation and accompanying neuritic outgrowth. Dominant negative nuclear FGFR1, which lacks the tyrosine kinase domain, prevents RA-induced differentiation while full-length nuclear FGFR1 elicits differentiation in the absence of RA. Immunoprecipitation and GST assays demonstrate that FGFR1 interacts with RXR, RAR and their Nur77 and Nurr1 partners. Conditions that promote these interactions decrease the mobility of nuclear FGFR1 and RXR in live cells. RXR and FGFR1 co-associate with 5′-Fluorouridine-labeled transcription sites and with RA Responsive Elements (RARE). RA activation of neuronal (*tyrosine hydroxylase*) and neurogenic (*fgf-2* and *fgfr1)* genes is accompanied by increased FGFR1, Nur, and histone H3.3 binding to their regulatory sequences. Reporter-gene assays show synergistic activations of RARE, NBRE, and NurRE by FGFR1, RAR/RXR, and Nurs. As shown for mESC differentiation, FGFR1 mediates gene activation by RA and augments transcription in the absence of RA. Cooperation of FGFR1 with RXR/RAR and Nurs at targeted genomic sequences offers a new mechanism in developmental gene regulation. J. Cell. Biochem. 113: 2920–2936, 2012.



**KEY WORDS:** FGFR1; RETINOIC ACID RECEPTORS; ORPHAN NUCLEAR RECEPTORS; EMBRYONIC STEM CELLS

Abbreviations: RA, Retinoic acid; at-RA, all trans-RA; CBP, CREB Binding Protein; EGFP, enhanced green fluorescent protein; YFP, yellow fluorescent protein; FGF-2, fibroblast growth factor-2; FGFR1, Fibroblast Growth Factor Receptor-1; FRAP, Fluorescent Recovery After Photobleaching; TK, tyrosine kinase; NLS, nuclear localization signal; INFS, Integrative Nuclear FGFR1 Signalling; ssTF, sequence specific transcription factors; RARE, RA-responsive elements; NurRE, Nur Responsive element; NBRE, NGFI-B response element; NR, Nuclear Receptor; mESC, mouse embryonic stem cells; hESC, human embryonic stem cells; NPC, neural progenitor cells; IR, immnunoreactivity; NB, neuroblastoma; HEK, human embryonic kidney; TH, tyrosine hydroxylase; α, antibody; GST, Glutathione-S-Transferase; ChIP, chromatin immunoprecipitation.

Additional supporting information may be found in the online version of this article.

Grant sponsor: NYSTEM; Grant numbers: C026415, C026714, C024355; Grant sponsor: NIH; Grant numbers: R21HL092398, R01HL103709.

*Correspondence to: Prof. Peter Claus, Institute of Neuroanatomy, Hannover Medical School, Carl-Neuberg-Str. 1, 30625 Hannover, Germany. E-mail: claus.peter@mh-hannover.de

*Correspondence to: Prof. Michal K. Stachowiak, Department of Pathology and Anatomical Sciences, State University of New York, 206A Farber Hall, 3435 Main Street, Buffalo, NY 14214. E-mail: mks4@buffalo.edu

Manuscript Received: 12 April 2012; Manuscript Accepted: 17 April 2012

Accepted manuscript online in Wiley Online Library (wileyonlinelibrary.com): 26 April 2012

DOI 10.1002/jcb.24170 • © 2012 Wiley Periodicals, Inc.

Systems biology postulates computational modules that integrate environmental information to control entry into the cell cycle and promote perpetual self-renewal by stem cells [Floettmann et al., 2011]. A universal signaling module, Feed-Forward-And-Gate, has recently been proposed to direct the post-mitotic development of neural cells through coordinated gene expression [Stachowiak et al., 1997b; Peng et al., 2001; Stachowiak et al., 2003a; Stachowiak et al., 2003b; Bharali et al., 2005; Fang et al., 2005; Stachowiak et al., 2007; Stachowiak et al., 2009; Stachowiak et al., 2011a; Stachowiak et al., 2011b]. Signals generated by diverse cell surface receptors are propagated through signaling cascades to sequence specific transcription factors (ssTF). In parallel, a newly synthesized FGF Receptor-1 (FGFR1) is released from the pre-Golgi membranes, which is enabled by an atypical FGFR1 transmembrane domain [Myers et al., 2003]. FGFR1 is transported to the nucleus by importin-β [Reilly and Maher, 2001] and "feeds forward" the membrane-generated signals directly to CREB binding protein (CBP), a common and essential transcriptional co-activator and gene-gating factor. The coupled activation of CBP by FGFR1, known as INFS, and cascade signal transduction to ssTF are responsible for cell differentiation [Fang et al., 2005; Stachowiak et al., 2007; Stachowiak et al., 2011b] (Note 1 in supplementary material).

A separate class of ontogenic regulators are dual function proteins which serve both as ssTF and nuclear vitamin or hormonal receptors but do not act via signaling cascades [Berrabah et al., 2011]. The pleiotropic developmental effects of retinoids are mediated by nuclear receptor (NR) subfamilies, RXR/RAR, which regulate transcriptional activity as homo/heterodimers by binding RA-responsive elements (RAREs) [Lefebvre et al., 2010]. In the absence of a ligand, RXR-RAR heterodimers are associated with corepressor complexes and inhibit gene activation. In response to ligand binding these heterodimers undergo conformational changes which facilitate transcription through the recruitment of co-activators and chromatin modifiers [Bastien and Rochette-Egly, 2004]. In the presence of all-trans RA (at-RA), when RAR is active, RXR functions as a "silent" partner and does not participate directly in transcriptional activation. However, when the 9cis-RA (9c-RA) ligand is available and both heterodimeric partners are active, RAR-induced dissociation of corepressors coupled with the cooperative recruitment of coactivators leads to synergistic activation of target genes [Germain et al., 2006]. Through histone modification, coactivators [p300/CBP and CARM-1] decompact local chromatin allowing the RXR-RAR heterodimers to recruit basal transcriptional machinery via an indirect interaction with the RNA Pol II holoenzyme [Duong and Rochette-Egly, 2011]. The increased accessibility of transcriptionally active DNA is further prolonged through the replacement of histone H3 by H3.3 [Elsaesser et al., 2010].

Given that RXR can partner with a variety of NRs (RARs, PPARs, LXRs, FXRs, TRs, VDR) [Bastien and Rochette-Egly, 2004; Germain et al., 2006; Lefebvre et al., 2010] it is evident that RXR heterodimers control many hormone/vitamin responsive genes. An important class of RXR partner includes members of the orphan NR subfamily, Nur77, Nurr1, and NOR-1, which are devoid of a ligand-binding domain and function as ssTF within multiple signaling pathways. Nur77, Nurr1, and NOR-1 are expressed in numerous tissues, including the brain, and play a role in cell proliferation, differentiation, and apoptosis [Watson and Milbrandt, 1990; Woronicz et al., 1994; Zetterstrom et al., 1997; Castillo et al., 1998; Saucedo-Cardenas et al., 1998; Backman et al., 1999; Kolluri et al., 2003]. Nur77 and Nurr1 form retinoid permissive heterodimers with RXRα and activate transcription by binding RAREs [Forman et al., 1995; Perlmann and Jansson, 1995]. In addition, Nur77 and Nurr1 activate transcription independently of RXR by binding DNA target motifs as monomers (NBRE) [Wilson et al., 1991] or as homo/heterodimers (NurRE) [Philips et al., 1997; Maira et al., 1999; Maira et al., 2003].

The present work describes how the developmental gene regulating functions of RAR, RXR, and Nur NR subfamilies are mediated in direct cooperation with FGFR1 and the INFS.

## MATERIALS AND METHODS

### PLASMIDS

Plasmids expressing high-molecular-weight (HMW; 23 kDa) and low-molecular-weight (LMW; 18 kDa) FGF-2 were described in [Claus et al., 2003]. FGFR1 mutants: FGFR1(TK-)-deleted tyrosine kinase domain, FGFR1(SP-/NLS)-signal peptide replaced with the nuclear localization signal (NLS) from the SV40 large T antigen, and FGFR1(SP-/NLS)(TK-) were described in[Peng et al., 2001, 2002]. The RARE-luciferase reporter, provided by Addgene (Addgene plasmid 13458; Cambridge, MA), has inserted eight repeat retinoic acid response elements (RARE) into the **pGL3** (pGL3-RARE-Luc) [Hoffman et al., 2006]. Plasmids NurRE3-Luc containing three Nur response elements and NBRE3-Luc containing three NGF binding response elements in minimal POMC gene promoter ($-34/+63$), Nur77 expressing pCMX vector were gifts from Dr. Jacques Drouin (Institut de Recherches Cliniques de Montrèal) [Maira et al., 1999; Maira et al., 2003]. The reference reporter plasmid, pGL4.70 [hRluc] promoterless, was from Promega Corp. (Madison, WI). The generation of pCAGGS-Nurr1-3xFlag is described in our separate submitted manuscript [Baron et al., 2012]. Briefly, pCAGGS-Nurr1-3xFlag was generated by inserting full length murine Nurr1 coding sequence (Nr4a2, GenBank NM_013613) PCR-amplified from the embryonic mouse brain cDNA, downstream and in frame with the 3XFlag in pCAGGS-3XFlag plasmid. Wild-type RXRα and Flag-RXRα (in pSG5, Stratagene) as well as GST-RARα (in pGEX-5 × 1, GE Healthcare Life Sciences) expression vectors have been described previously [Qiu et al., 2007, 2010]. Fluorescent plasmids: Chimerical FGFR1 with C-terminal EGFP [Myers et al., 2003] and RXRα-EYFP were described previously [Qiu et al., 2007, 2010].

### ANTIBODIES

Polyclonal αFGFR1 (C-terminal, sc-121), αGFAP (sc-6171), αTH (sc-7874), CBP (sc-369), αRXR (ΔN 197, sc-773), αRAR (M-454, sc-773), αNurr1/77 (sc-990), αNurr1 (sc-991), αNurr77 (sc-5569), and αGADPH (sc-137179) were purchased from Santa Cruz Biotechnology (Santa Cruz, CA). The N-terminal αFGFR1 mcAb6 was described in [Hanneken et al., 1995]. Monoclonal mouse αFGFR1 (N-terminal)(ab823), αβIII-tubulin(ab18207), αOct4 (ab18976),

αH3.3 (ab62642), αHistone H3 (tri methyl K4, ab8580) were purchased from Abcam (Cambridge, MA). Rabbit αMatrin-3 Ab (A300–591A) was from Bethyl Laboratories (Montgomery, TX). Rat αBrdU Ab (MCA2060) were purchased from AbD Seretec (Raleigh, NC). αFlag (F3165) was from Sigma-Aldrich (St. Louis, MO). Mouse (X0931) and rabbit IgG (X0903) from Dako (Carpinteria, CA). Specificity of immunostaining was ascertained with control reactions in which the primary Ab was omitted or replaced with preimmune sera or by neutralizing the antibody with cognate peptide [Stachowiak et al., 1996a; Somanathan et al., 2003].

## CELL CULTURE, TRANSFECTION, AND NEURITE OUTGROWTH

**Mouse ESC culture and differentiation.** The undifferentiated growth method of the E14Tg2a mESC was previously described including the use of LIF supplemented growth media containing serum [Kehoe et al., 2008]. Experiments were performed in LIF-free mESC monolayers. Cells were treated with 1 μM at-RA or vehicle (0.002% DMSO). Human ESC H9 cell line from WiCell Research Institute (Madison, WI) were used for these experiments under the approval of the Committee for Stem Cell Research Oversight at SUNY-Buffalo. The culture conditions have been described [Lock and Tzanakakis, 2009] and involved growing hESC on a feeder layer of mouse embryonic fibroblasts.

Human Neural Progenitor Cells (HNPC), from the CNS of 12–18 week embryos (CloneExpress) were cultured as previously [Somanathan et al., 2003]. Human neuroblastoma cell line BE(2)C was cultured in Dulbecco modified Eagle medium/Nutrient Mixture F-12 (DMEM/F-12, Gibco) and Human Embryonic Kidney (HEK) cells in RPMI Medium 1640 (Gibco), both supplemented with 10% (v/v) fetal bovine serum, 100U/ml penicillin/0.1 mg/ml streptomycin and non-essential amino acid. All cells were cultivated in a humidified atmosphere at 37°C and 5% $CO_2$. Cell transfections were performed using Lipofectamine 2000 (Invitrogen).

The at-RA-induced outgrowth of β-III-tubulin-expressing neurites and the effects of dominant negative and constitutively active FGFR1 were analyzed by transfection of mESC with two plasmids, one expressing recombinant FGFR1 or control B-gal and the second expressing EGFP to mark the transfected cells. Twenty-four hours after transfection cultures were switched to LIF-depleted medium with or without (control) 1 μM at-RA for an additional 4 days. Cells were then immunostained with αβIII Tubulin (+goat-anti-rabbit Alexa568) and imaged using a CCD camera. Cell bodies and EGFP fluorescent extensions cells were outlined using the ImageJ freehand tracing tool. We used a standardized method in which β-III-tubulin positive processes that were 1× longer than the cell width and displayed neurite-like morphology were measured. Cells with the shorter protrusions were scored as having a neurite length equal to zero. This method is based on earlier publications [Stachowiak et al., 2003a; Fang et al., 2005; Zhang et al., 2005].

## DUAL LUCIFERASE ASSAYS

The assays were performed with the dual luciferase reporter system (Promega Corp., Madison, WI). Luminescence measurement was performed on BioTek Plate Reader. All data were calculated as the ratio of firefly to Renilla luciferase activity. Experiments were repeated 2–4 times and each was performed in quadruplicate.

## CELL FRACTIONATION AND WESTERN BLOTTING

Cells were fractionated as described in [Stachowiak et al., 1996a; Peng et al., 2001] and the purity of fractions was verified in previous studies which showed less than 5% of the total cellular activity of 5′ nucleotidase (plasma membrane marker), and less than 2% of the total activity of acid phosphatase (lysosomal marker; Stachowiak et al., 1996ab, 1997a). Furthermore the cell membrane associated biotinylated FGFR1 or FGFR1(TK-) were not detectable in the nuclear fraction [Peng et al., 2002].

Equal amounts of proteins of the cytoplasmic or nuclear fractions were loaded and separated on SDS–7.5% polyacrylamide gel and transferred to PVDF (Millerport). Blots were probed with the appropriate antibodies and the immune complexes revealed by chemiluminescence using SuperSignal Femto Maximum Sensitivity Substrate (Pierce) and Fuji chemiluminescence imager. Equal protein content in individual lanes was verified by Ponceau S Red staining (Fig. 1a), which reveals different proteins present in cytoplasmic and nuclear fractions. In addition, we immunoblotted for GADPH, which is present predominantly in the cytoplasm but also in the nucleus [Sen et al., 2008; Kornberg et al., 2010] (Fig. 3b), and for αMatrin, which is predominantly in the nucleus (Fig. 3b, S1a).

## CO-IMMUNOPRECIPITATION

Nuclear and Cytoplasmic fractions are diluted 1:2 in RIPA buffer (137 mM NaCl, 20 mM Tris-HCl pH 7.5, 25 mM NaF, 2 mM EDTA, 1% TX100, 1% (w-v) sodium Deoxycholate, 2 mM DTT, 1 mM PSM and 10 μM protease inhibitor). 750 μg of protein is incubated with 2 μg of antibody overnight in 4 c. Invitrogen Dynabeads are used for pull down following the indirect protocol. The immunoprecipitated proteins were denatured at 95°C in sample-buffer.

## GLUTATHIONE-S-TRANSFERASE (GST) PULL DOWN

GST and GST-RARα fusion protein were expressed in *E. coli* DH5α and the crude lysates were prepared as described in [Peng et al., 2001; Peng et al., 2002]. NB cells were transfected with FGFR1-Flag and Nur77. Forty eight hours after transfection the nuclear NB cell lysates were selected with GST or GST-RAR beads and resolved by 8% SDS–PAGE for immunoblotting.

## FRAP

FRAP analyses of transiently transfected FGFR1-EGFP [Dunham-Ems et al., 2006, 2009] and RXR-YFP [Dong et al., 2004] were performed as previously described. The transfected recombinant proteins were expressed at the levels comparable to endogenous proteins [Dunham-Ems et al., 2006, 2009]. The intensities of FGFR1-EGFP fluorescence or RXR-YFP in individual transfected cells were similar and, as in our previous studies [Dunham-Ems et al., 2006, 2009], cells were randomly selected for FRAP measurements. Imaging was performed in 35 mm glass bottom dishes (MedTek Corp.) using Zeiss 510 Meta confocal laser scanning microscope with an incubation chamber (37°C and 5% $CO_2$, Pecom) an oil immersion objective (63×, 1.4 NA), a zoom magnification (twofold), the 488-nm argon laser line for GFP, and 513-nm for

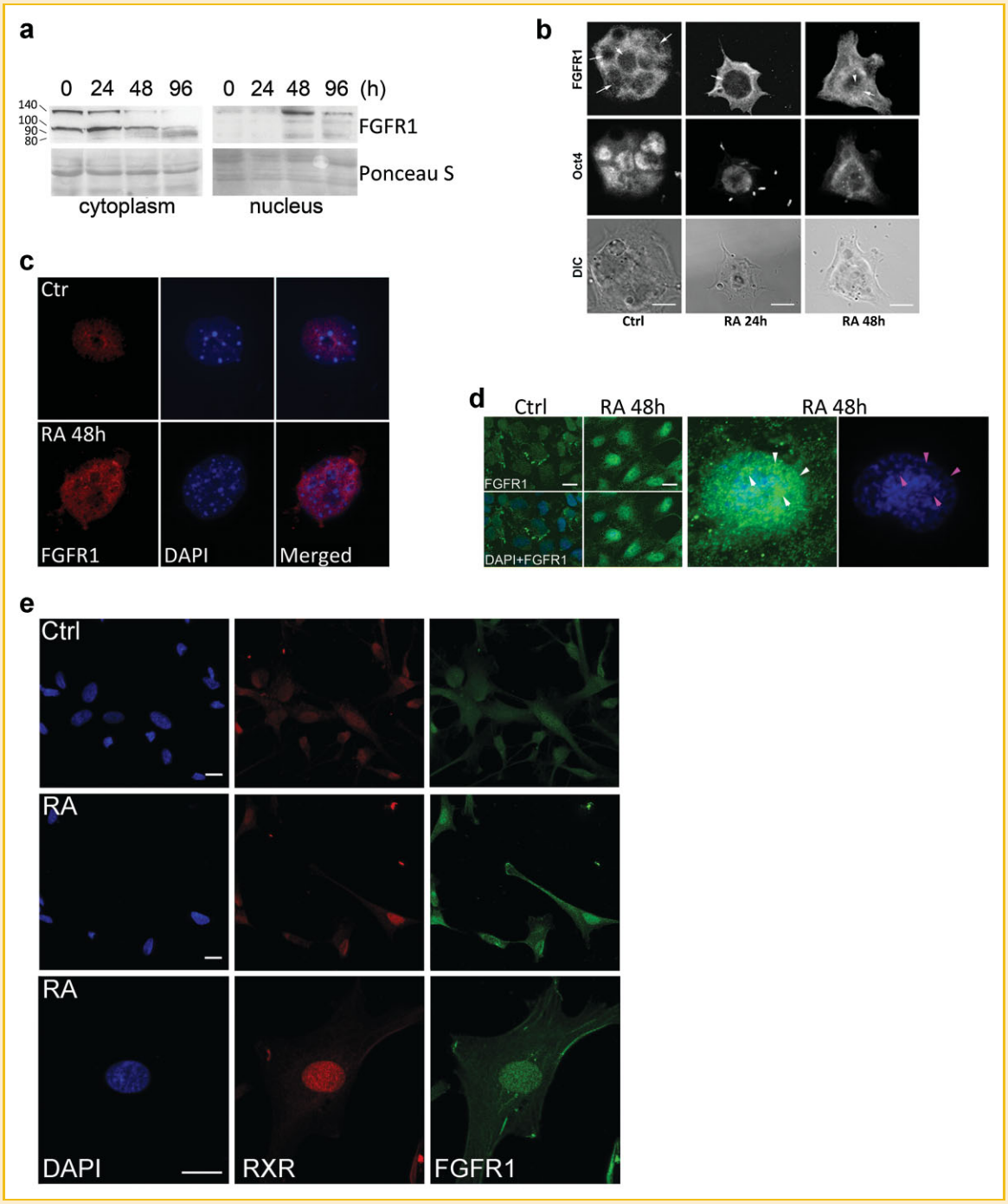


Fig. 1. Nuclear accumulation of FGFR1 is a common response to at-RA in stem and progenitor cells. a: mESC [Kehoe et al., 2008] were treated with 1 μM at-RA for an indicated time period or maintained in LIF-depleted control medium. All dishes were harvested at the same time and nuclear and cytoplasmic fractions were isolated, electrophoresed (40 μg protein/lane), and immunoblotted with αFGFR1 McAb6 [Stachowiak et al., 1997a]. Cytoplasmic and nuclear FGFR1 are represented by 140, 100, 90, and 80 kDa FGFR1 which correspond to different degrees of receptor glycosylation [Stachowiak et al., 1997b; Myers et al., 2003]. The at-RA induced changes are evident relative to equal protein content in individual lanes stained with Ponceau S Red. Normalization to GADPH (Fig. 3b) or predominantly nuclear αMatrin (Fig. 1d, S1A) confirms the at-RA induced nuclear FGFR1 accumulation. The same results were obtained in three independent experiments (not shown). b: mESC treated with 1 μM at-RA for 24 or 48 h and co-immunostained with αFGFR1 McAb6 [Hanneken et al., 1995] (+ goat-anti-mouse Alexa 488) and rabbit αOct4 (+ goat-anti-rabbit Alexa 568). Confocal sections through the middle of the cell (cytoplasm and nuclei) are shown. Following at-RA treatment we observed nuclear accumulation of FGFR1 after 48 h which is accompanied by a depletion of the pluripotency associated protein Oct4. Nuclear accumulation of FGFR1 was also verified using different mouse monoclonal αFGFR1 (ABCAM; Fig. 1d,e) and polyclonal C-term αFGFR1(ABCAM; Fig. 1c). c: DNA staining with DAPI reveals FGFR1 exclusion from condensed heterochromatin (strong DAPI) and colocalization with less dense euchromatin (weak DAPI). mESC treated with 1 μM at-RA for 48 h or maintained in LIF-depleted control medium and immunolabeled with C-term αFGFR1 (ABCAM) (+ goat-anti-rabbit Alex488) Confocal sections through the nuclei, above the cytoplasm, are shown. d: Human ESC [Lock and Tzanakakis, 2009] were incubated with or without (control) 1 μM at-RA for 48 h and immunolabeled with N-terminal αFGFR1 (ABCAM) (+ goat-anti mouse-Alex488). Arrowheads point to weakly stained (DAPI) euchromatin regions with high FGFR1-IR after at-RA stimulation. e: Human NPC were incubated with or without (control) 1 μM at-RA for 48 h and immunolabeled with N-terminal αFGFR1 (ABCAM) (+ goat-anti mouse-Alex488, green) and αRXR (+goat-anti rabbit- Alexa568, red). Nuclear DNA was stained with DAPI. RXR-IR is located both in the nucleus (predominantly) and in the cytoplasm. Nuclear accumulation of FGFR1 is observed after at-RA treatment. Bar size: 20 μm.

YFP. Intensity of fluorescence in individual transfected cells were similar, and cells were randomly selected for FRAP measurements. FRAP images for R1-EGFP were acquired every 0.5 s for 30 s, then every 2 s for an additional 1 min, and finally every 5 s for 1.5 min. FRAP images for RXR-YFP were acquired every 0.5 s for 10 s, then every 2 s for an additional 30 s, and finally every 5 s for another 1 min. The acquired images of a minimum of 15 cells/condition were collected and analyzed using the standard microscope software. The laser output for FRAP-bleaching was set to 100% and bleached regions chose were of the same size. The images were used only for subsequent analysis when the relative fluorescence intensity (RFI) after bleaching was up to 50% in relation to the fluorescence intensity before bleaching. Data were corrected for background intensity and for the overall loss in total intensity as a result of the bleach pulse and the imaging scans. The kinetic constant (k) and the mobile fraction for a FRAP experiment were calculated by Fcalc software by fitting one or two exponential curve to the corrected data using a least square fit [Dunham-Ems et al., 2006]. The one function FRAP recovery fit for RXR-YFP was calculated as $F_{\infty} = A(1\text{-}e^{kt})$. The two-phase exponential FRAP recovery of FGFR1-EGFP was calculated as $F_{\infty} = A_1(1\text{-}e^{k1t}) + A_2(1\text{-}e^{k2t})$; A is the mobile fraction and k is the kinetic constant. In addition to these parameters the half time, $t_{1/2}$, of the reaction is given. The value of the half time, $t_{1/2}$ recovery was calculated with the following formula, $t_{1/2} = ln(0.5)/k$. Microsoft EXCEL and SPSS were used for plotting of the data and statistical analysis. ANOVA tests were applied to analyze differences among recovery half-times ($t_{1/2}$), populations of mobile FGFR1-EGFP or RXR-YFP, and the effects of cotransfected proteins.

## IMMUNOCYTOCHEMISTRY

Cells were fixed with 4% paraformaldehyde and permeabilized with 1% Triton X-100. Appropriate primary and secondary antibodies (described in the legends of figures) as well as DAPI were applied for immune-staining [Somanathan et al., 2003; Fang et al., 2005]. Immunostaining was observed using either Zeiss Axioimager fluorescence microscope with an 40× oil objective or Zeiss 510 Meta confocal laser scanning microscopes (Thornwood, NY) with an oil immersion objective (63 ×, 1.4 NA), the 488-nm argon laser line, the 561-nm DPSS laser line, 633-nm HeNe laser line and Chameleon laser line (Coherent Inc.) for DAPI. The border of the nuclei was identified in DAPI-stained cells and in phase-contrast images. The acquired images and co-localized images were analyzed using ImageJ imaging software and its plug-in RG2B co-localization or JACoP. For that purpose the original 16-bit images were used. Confocal images were also exported as original 16 bit images with the size of 0.093 μm/pixel × 0.093 μm/pixel. The intensity of immunofluorescence in each channel in individual cell was normalized to similar level. The threshold for determining co-localization was set as the mean of immunofluorescence of the region of interest. The specificity of FGFR1 immunostaining was demonstrated as previously [Stachowiak et al., 1996b; Stachowiak et al., 1997a; Fang et al., 2005; Dunham-Ems et al., 2006; Dunham-Ems et al., 2009] by several observations: Staining was not observed when the primary antibody was omitted or replaced with preimmune serum (not shown); similar nuclear cytoplasmic localization was observed by using four antibodies targeting different FGFR1 epitopes and by detection of transfected FGFR1–EGFP and FGFR1–Flag using native fluorescence and αFlag. The presence and changes in the levels of nuclear FGFR1 immunoreactivity were confirmed by western blot analysis of FGFR1 in subcellular fractions.

## mRNA LEVEL DETERMINATION USING QUANTITATIVE PCR

Total RNA was isolated from 35 mm plates of mESC cultures using Trizol. cDNA synthesis was carried out using 1 μg RNA and the iScript cDNA Synthesis Kit (Bio-Rad; Hercules CA). One tenth of the synthesized cDNA was used as the template for real-time PCR. Twenty-five microliters real time PCR reactions were performed on the BioRad MyiQ Cycler with iQ SYBR Green Supermix (Bio-Rad). RT qPCR using the amplification cycles: Initial denaturation for 8 min at 95°C, followed by 35× cycle 2 (denaturation for 15 s at 95°C and annealing for 1 min at 60°C). Melt curve data collection was enabled by decreasing the set point temperature after cycle 2 by 0.5°C. The specificity of amplicons was confirmed by generating the melt curve profile of all amplified products. Gene expression was quantified as described [Pfaffl, 2001].

## ChIP ASSAYS

Cells grown on a 60 mm plate were cross-linked with 1% formaldehyde (Sigma, St Louis, MO) at 37°C for 10 min, rinsed twice with cold phosphate-buffered saline, and harvested in phosphate-buffered saline with protease inhibitors by 5 min centrifugation at 2,000*g*. ChIP was performed according manufacturer's instructions (Millipore,Temecula, CA 92590). Genomic DNA and transfected RARE-luciferase was precipitated with ethanol and after treatment with RNase A and proteinase K, purified using Qiagen PCR purification kit. PCR was then performed on the immunoprecipitated genomic DNA with primers for the response element containing regions of *fgfr1*, *fgf-2*, and *th* genes and control *Prm1* gene. All primers amplifying these promoter regions and 8xRARE in RARE-luciferase are shown in Table S1.

## qPCR ANALYSIS OF ChIP

qPCR was used to determine relative amount of specific loci in IP, Input, and IgG(Preimmune) samples. qPCR was performed using iQ SYBR Green Supermix (Bio-Rad) on a Bio-Rad iCycler. Three microliters of Chip DNA and a 1:100 Dilution of input DNA was used in duplicate reactions. The *Prm1* gene was used as an internal control to normalized quantification in qPCR reactions. Data are expressed as IP/Input where $\Delta\Delta CT = (Ct_{IP\ geneX} - Ct_{IP\ prm1}) - (Ct_{Input\ geneX} - Ct_{Input\ prm1})$.

## STATISTICAL TESTS

Microsoft EXCEL and SPSS were used for plotting of the data and statistical analysis. For all data ANOVA was used and significant differences were analyzed by L.S.D. or Tukey posthoc tests. Interactions between factors were analyzed using 2-Way ANOVA.

## RESULTS

### NUCLEAR ACCUMULATION OF FGFR1 IS A COMMON RESPONSE TO at-RA IN STEM AND PROGENITOR CELLS

at-RA applied to multi-potent mouse (m)ESC induces concentration and time dependent differentiation of neuronal, cardiac, myogenic, adipogenic and vascular smooth muscle cells, (reviewed in [Rohwedel et al., 1999]). Typically, 1 nM at-RA promotes cardiomyocytic differentiation while 1 μM at-RA converts mESC into neurons [Fraichard et al., 1995; Wobus et al., 1997; Kehoe et al., 2008]. Furthermore, at-RA promotes neuronal differentiation in multi-potent mouse and human (h) embryonic stem cells (ESC) and neural progenitor cells (NPC) [Morriss-Kay and Sokolova, 1996; Rohwedel et al., 1999]. To determine whether at-RA activation incorporates the INFS mechanism we analyzed the expression and subcellular localization of FGFR1 in mESC, hESC, and hNPC.

In control non-treated mESC the cytoplasmic fraction expresses predominantly 100 and 140 kDa high molecular weight FGFR1 (Fig. 1a), known to represent different degrees of receptor glycosylation [Stachowiak et al., 1997b]. Both forms are depleted in the cytoplasm after 2 or 4 days of at-RA treatment while an increase in nuclear 100 and 140 kDa FGFR1 is observed. The reverse changes in cytoplasmic and nuclear FGFR1 levels illustrate lack of cross-contamination in isolated fractions.

In addition, at-RA increases both cytoplasmic and nuclear 80–90 kDa FGFR1, which are precursors of the hyperglycosylated forms [Dunham-Ems et al., 2006]. Consistent with these biochemical results, in non-treated mESC, FGFR1 immnunoreactivity (IR) is primarily cytoplasmic. After 2 days of at-RA treatment we observed a marked increase in nuclear FGFR1 (Fig. 1b) which remained elevated for at least 1 week after treatment (not shown). In addition, there is a parallel depletion of the pluripotent marker Oct4 in cells which accumulate nuclear FGFR1 (Fig. 1b). Confocal microscopy reveals nuclear FGFR1 is excluded from condensed heterochromatin but is enriched at euchromatin-like sites (Fig. 1c). Treatment with at-RA also induces a similar nuclear accumulation of FGFR1 in human pluripotent ESC (Fig. 1d), human brain multi-potent NPC (Fig. 1e), differentiating neuroblastoma cells (Fig. 3b) as well as in rat hippocampal progenitor cells (not shown). We conclude that the nuclear accumulation of FGFR1 represents a common response of developing cells to at-RA stimulation.

Shorter at-RA treatment (24 h) has no detectable effect on FGFR1 proteins (Fig. 1a,b). However, in the presence of leptomycin B, which blocks nuclear export, nuclear accumulation of FGFR1 is detected within 4–24 h indicating an early at-RA-induced FGFR1 nuclear translocation (Fig. S1A).

### NUCLEAR FGFR1 MEDIATES RA-INDUCED NEURONAL-LIKE DIFFERENTIATION OF mESC

We verified earlier findings that at 1 μM at-RA promotes mESC development along the neuronal lineage while instructing against glia cell development [Kehoe et al., 2008] (Fig. 2a) (Fig. S1B, C; Note 2 in supplementary material). To determine whether endogenous FGFR1 is involved in at-RA-induced outgrowth of βIII-tubulin expressing neurites we used an established neurite outgrowth assay [Fang et al., 2005]. In a loss of function experiment we transfected mESC with dominant negative mutants of FGFR1, which lack the tyrosine kinase domain, form non-functional dimers with the endogenous receptor and compete with wild type FGFR1 for its nuclear targets [Fang et al., 2005]. FGFR1(TK-) localizes to cytoplasmic membranes and cell nuclei. FGFR1(SP-/NLS)(TK-), in which the signal peptide is replaced with a nuclear localization signal, functions exclusively in the nucleus [Peng et al., 2001; Peng et al., 2002; Somanathan et al., 2003; Fang et al., 2005]. Cells transfected with a control vector display short processes, however, when treated with at-RA the processes elongate, with one process becoming 4–5 times longer than in the absence of at-RA and display distinct βIII-tubulin immnunoreactivity (IR) (Fig. 2b). The dominant negative receptors have no significant effect on neurite length in non-stimulated cells compared to control transfected mESC (Fig. 2b). In contrast, cells transfected with FGFR1(TK-) or FGFR1(SP-/NLS)(TK-) fail to extend βIII-tubulin-IR neurites in response to at-RA even after prolonged treatment (7 days, not shown). In a gain of function experiment, mESC transfected with full length nuclear FGFR1(SP/-NLS) [Peng et al., 2001, 2002; Somanathan et al., 2003], which contains a functional TK domain, display a marked fivefold elongation of βIII-tubulin expressing neurites indistinguishable from that induced by at-RA (Fig. 2b). The effects of FGFR1 on neurite outgrowth are statistically significant and summarized in Figure 2b. These experiments indicate that nuclear FGFR1 is a necessary mediator of at-RA-induced morphological differentiation of mESC and sufficient to induce neurite outgrowth in the absence of at-RA (Note 2 in supplementary material). In addition, FGFR1(SP/-NLS)-differentiated mESC seize to proliferate (incorporate BrdU) (not shown), as found previously in other stem-like cells [Fang et al., 2005].

### INTERACTION OF FGFR1 WITH RETINOID RECEPTORS

Based on the requirement of FGFR1 in the differentiation actions of at-RA, we next studied whether interaction between FGFR1 and RA receptors occurs in mESC and other cells. Double immunostaining followed by confocal microscopy reveal the co-localization of FGFR1-IR with RAR-IR or RXR-IR pixels (Fig. 3a). Co-localized FGFR1-RAR and FGFR1-RXR are observed in the cytoplasm, sub-plasma membrane region, and within the discrete nuclear domains (Fig.S2A,B). The interaction between endogenous cytoplasmic and nuclear FGFR1 and RXR or RAR was established by co-immunoprecipitation (co-IP) (Fig. 3b). Both the hypo-glycosylated (80–100 kDa) and hyper-glycosylated (110–140 kDa) nuclear and the cytoplasmic forms of endogenous FGFR1 are immunoprecipitated by αRAR or αRXR but not by rabbit IgG (control). FGFR1 precipitated with an antibody against the C-terminal of FGFR1 is detected by an N-terminal monoclonal αFGFR1, confirming that cytoplasmic and nuclear FGFR1 forms represent non-truncated receptors [Stachowiak et al., 1996a; Stachowiak et al., 1996b; Dunham-Ems et al., 2006].

RAR-FGFR1 and RXR-FGFR1 interactions were also shown by reverse co-IP of cytoplasmic and nuclear RAR and RXR with αFGFR1 (Fig. 3c). Both RAR and RXR are immunoprecipitated by αRAR and αRXR further demonstrating the formation of the RXR/RAR heteromeric complexes. The interaction between endogenous

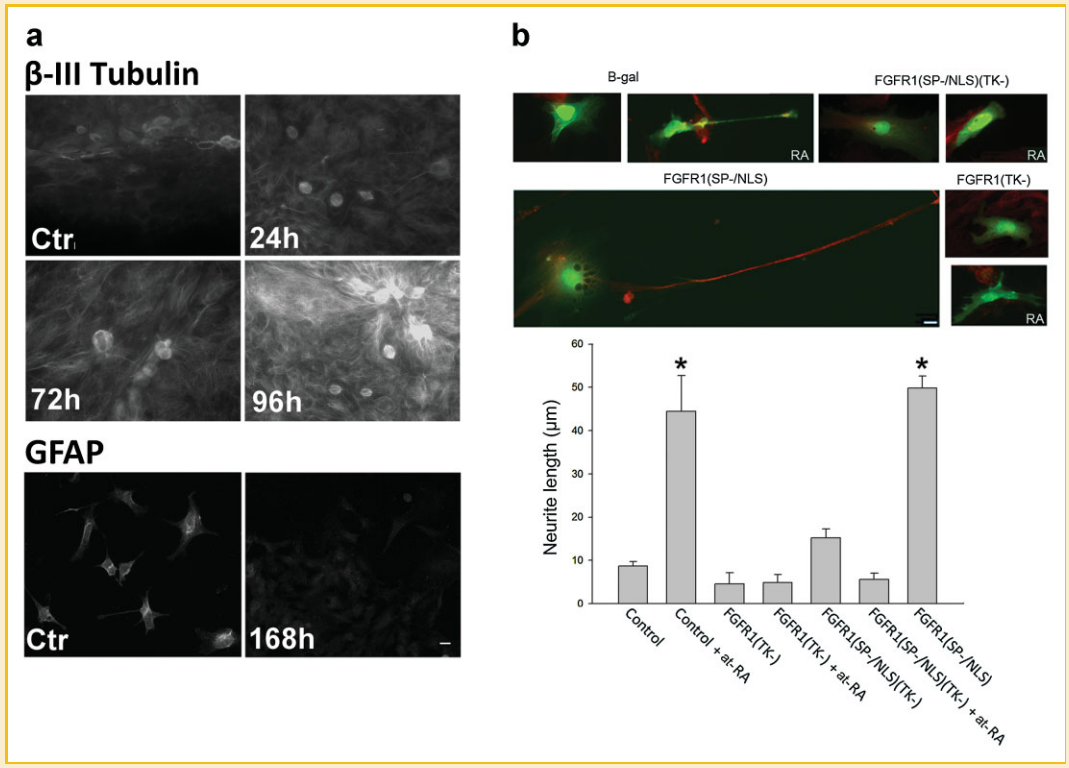


Fig. 2. Neuronal-like differentiation of mESC by at-RA. a: Control cells have short processes and display relatively weak staining with αβIII-Tubulin (+ goat-anti-rabbit Alexa 568). Treatment with at-RA leads to a gradual outgrowth of neurites with intensified βIII-Tubulin staining. Control mESC display weak αGFAP (+ goat-anti-rabbit Alexa 568) immunostaining which is no longer observed after 196 h of at-RA treatment (Fig. 1c). Typically no cells with apoptotic nuclei are observed in these conditions arguing against the at-RA induced loss of astrocytes or their precursor. b: The at-RA-induced outgrowth of β-III-Tubulin containing neurites in mESC is inhibited by dominant negative nuclear FGFR1. mESC were transfected with two plasmids, one expressing recombinant FGFR1 or control B-gal expressing vector and the second expressing EGFP. EGFP diffuses throughout the cell permitting visualization of the entire neuritic network. More than 90% of cells co-express transfected plasmids as reported in previous studies [Horbinski et al., 2001; Stachowiak et al., 2009]. Twenty-four hours after transfection cultures were switched to LIF-depleted medium with or without (control) 1 μM at-RA for an additional 4 days. Cells were then immunostained with αβIII Tubulin (+goat-anti-rabbit Alexa568) and imaged using a CCD camera. The longest process in an individual transfected (green) cell was measured and we observed morphological changes in fluorescent cells. Cells transfected with a B-gal vector and treated with at-RA exhibit a fivefold increase in the average neurite length ($P < 0.001$). In contrast, cells transfected with FGFR1(TK−) or FGFR1(SP−/NLS)(TK−) display no significant changes in average neurite length in the presence of at-RA. In the absence of at-RA, the average neurite outgrowth induced by active nuclear FGFR1(SP-/NLS) is similar to the at-RA induced outgrowth. The results are from four experiments, in which 40–80 cells per treatment were analyzed. ANOVA shows significant effects of at-RA and transfected plasmids as well as the interaction between at-RA and FGFR1(TK-) or FGFR1(SP-/NLS)(TK-) ($P = 0.001$). The differences are identified by Tukey's post-hoc test. Bar size = 20 μm.

FGFR1 and RXR or RAR is not limited to in vitro cultures and is also observed in the developing mouse brain (Fig.S2C). Hence, FGFR1 interaction with retinoid receptors appears to represent a general developmental phenomenon.

To further confirm the interactions between FGFR1 and RXR/RAR we utilized two cell lines, neuroblastoma NB2A (NB) and human embryonic kidney (HEK), which can be effectively transfected with these recombinant receptors. NB cells express endogenous FGFR1 as well as endogenous RAR and RXR that are readily detectable in the nucleus, whereas the levels of cytoplasmic RAR and RXR are below detection limits (not shown). Treatment of NB with at-RA increases nuclear FGFR1 as well as nuclear RAR (Fig. 3d, top part). Both αRAR and αCBP, an established FGFR1-binding transcription co-activator, precipitate endogenous FGFR1 from nuclear extracts of at-RA treated NB cells (Fig. 3d, bottom part). NB cells co-transfected with FGFR1 and RAR or RXR show increased FGFR1 co-immunoprecipitation (Fig. 3e). In reverse pull down experiments, RAR is immunoprecipitated by αRAR or αRXR as well as αFGFR1 (Fig. 3f) and RXR is immunoprecipitated by αFGFR1 from both nuclear and cytoplasmic fractions (Fig. 3g).

Finally, in HEK cells, which express endogenous RAR and RXR we detect little or no endogenous FGFR1, whereas after FGFR1 transfection the receptor was detected in both the nucleus and cytoplasm (Fig. 3h). Transfection of FGFR1-flag or RXR-flag in HEK cells provides further evidence for associations of retinoid receptors with FGFR1 (Fig. 3i,j). Immunoprecipitation of FGFR1 also co-precipitates RXR and vice versa (Fig. 3j). Considered together, these studies establish clear evidence for robust interaction between FGFR1 and retinoid receptors in variety of cell types.

## NUCLEAR MOBILITY OF RXR AND FGFR1 IN LIVE CELLS IS INFLUENCED BY CONDITIONS THAT PROMOTE THEIR MUTUAL INTERACTION

The kinetic mobility of nuclear RXR is reduced by interactions with nuclear partner proteins [Dong et al., 2004; Feige et al., 2005]. Therefore, we examined whether the intracellular mobility of RXR

is influenced by FGFR1. Chimeric RXR-YFP was co-transfected with control β–galactosidase (B-gal) or FGFR1(SP-/NLS) to analyze intra-nuclear FGFR1-RXR interactions. FRAP recovery curves were fitted to a single-order exponential function. At-RA induces a threefold decrease in the recovery rate and transfected FGFR1(SP-/NLS) induces a similar but less pronounced (50%) decrease (Fig. 4a). To further analyze these changes, cells in each treatment condition were assigned to one of three RXR-YFP recovery groups: Fast ($t1/2 < 1$ s), moderate ($t1/2 = 1–2$ s), and slow ($t1/2 > 2$ s). Figure 4a shows the percentage of cells in each group within different treatment categories. At-RA decreases the number of "fast" and "moderate" cells while increasing the "slow" cells. The effect of co-transfected FGFR1(SP-/NLS), which includes the depletion of fast and expansion of slow cells, is similar but less pronounced than that observed with at-RA treatment.

Mobility of transfected chimerical FGFR1–EGFP in the cell nucleus is determined by interaction with nuclear proteins and structures [Dunham-Ems et al., 2009]. Earlier FRAP analyses of transiently transfected FGFR1-EGFP revealed three nuclear FGFR1 populations: (i) A fast mobile ($t1/2 < 1$ s) which represents a freely

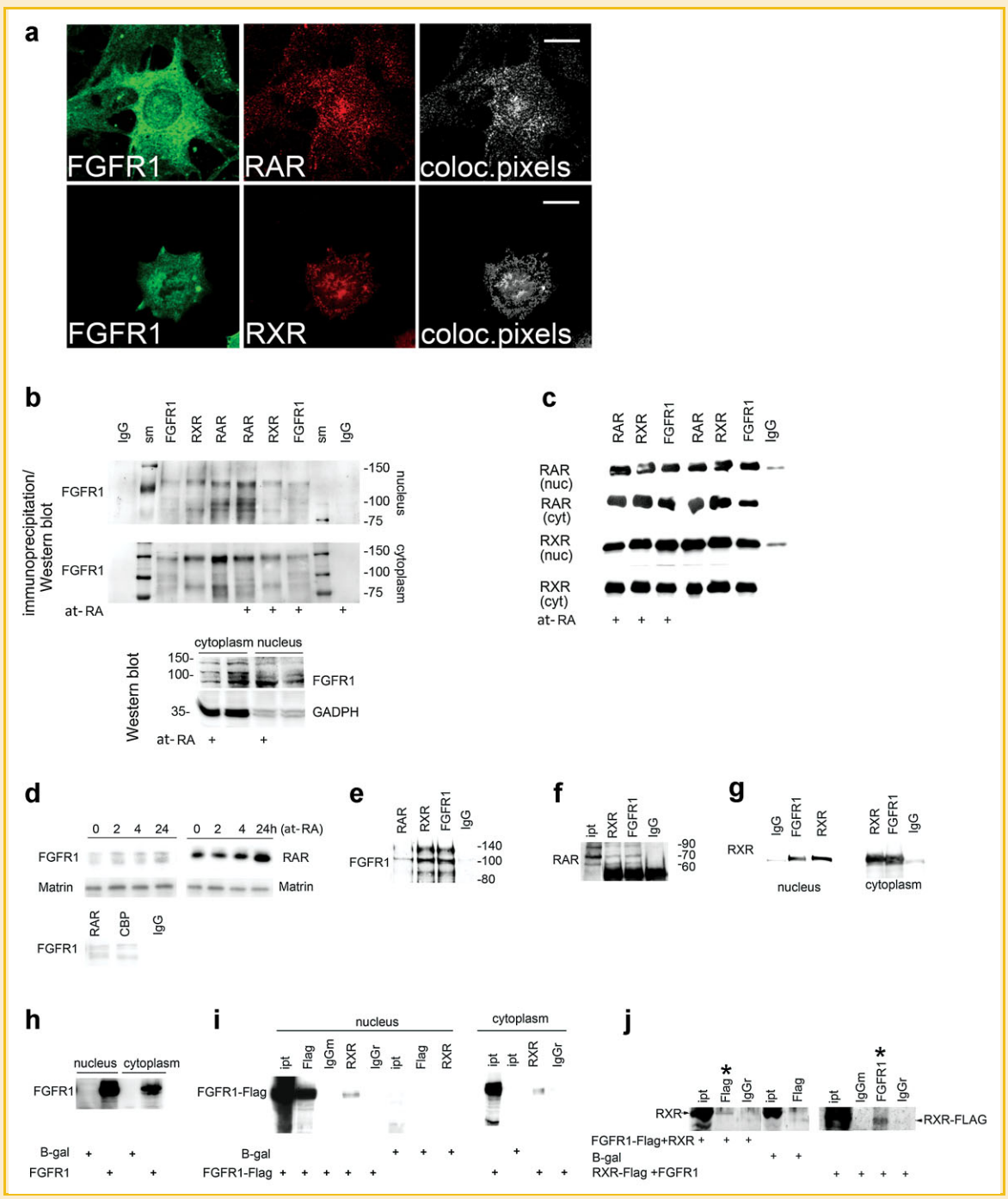

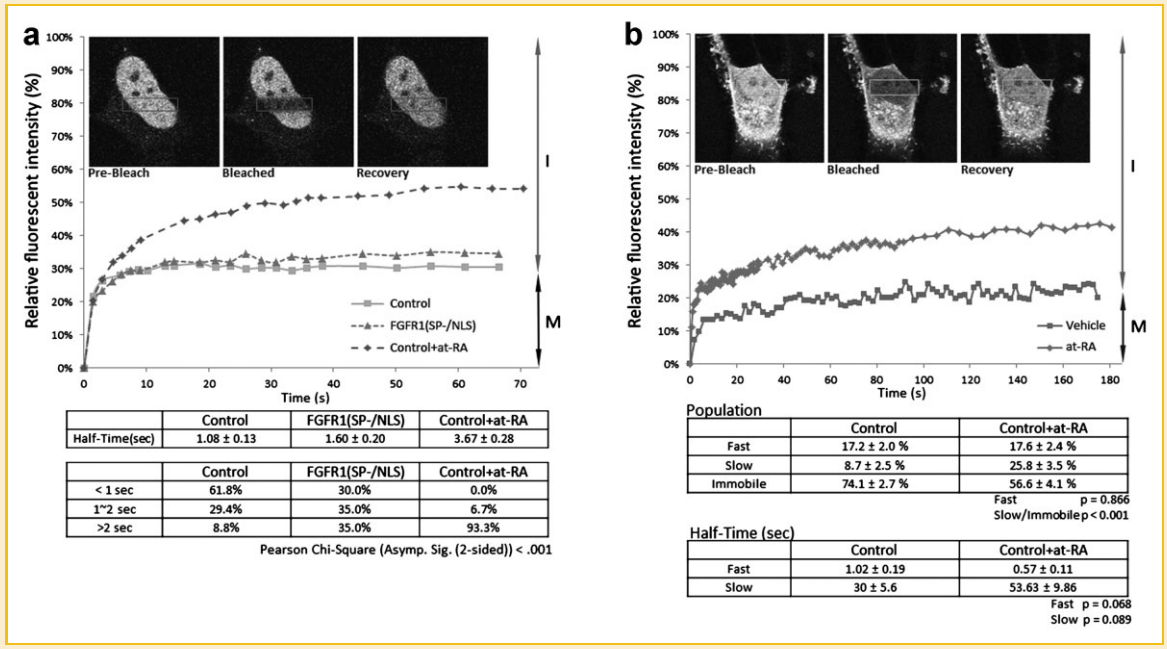


| | Control | FGFR1(SP-/NLS) | Control+at-RA |
|---|---|---|---|
| Half-Time(sec) | 1.08 ± 0.13 | 1.60 ± 0.20 | 3.67 ± 0.28 |

| | Control | FGFR1(SP-/NLS) | Control+at-RA |
|---|---|---|---|
| < 1 sec | 61.8% | 30.0% | 0.0% |
| 1~2 sec | 29.4% | 35.0% | 6.7% |
| >2 sec | 8.8% | 35.0% | 93.3% |

Pearson Chi-Square (Asymp. Sig. (2-sided)) < .001

Population

| | Control | Control+at-RA |
|---|---|---|
| Fast | 17.2 ± 2.0 % | 17.6 ± 2.4 % |
| Slow | 8.7 ± 2.5 % | 25.8 ± 3.5 % |
| Immobile | 74.1 ± 2.7 % | 56.6 ± 4.1 % |

Fast p = 0.866
Slow/Immobile p < 0.001

Half-Time (sec)

| | Control | Control+at-RA |
|---|---|---|
| Fast | 1.02 ± 0.19 | 0.57 ± 0.11 |
| Slow | 30 ± 5.6 | 53.63 ± 9.86 |

Fast p = 0.068
Slow p = 0.089

Fig. 4. FRAP mobility of nuclear RXR and FGFR1 (Note 3 in supplementary material). a: RXR-YFP [Qiu et al., 2010] was transfected into NB cells with FGFR1(SP-/NLS) or an empty pcDNA 3.1 vector. Twenty-four hours after transfection, some of the pcDNA3.1 cultures were treated with 1 μM at-RA for an additional 24 h and during subsequent imaging. Examples of the RXR-YFP-expressing cells before and after photobleaching are shown. RXR-YFP was expressed predominantly in nucleus. FRAP mobility of RXR-YFP in NB cells were analyzed by fitting to one-exponential function. The graph shows the percentage of mobile cell populations of RXR-YFP: Fast recovering ($t_{1/2} < 1$ s), moderate ($t_{1/2} = 1$–2 s), and slow recovering ($t_{1/2} > 2$s). Treatment with at-RA reduces the fast and moderate cell populations while increasing the slow population. The FGFR1(SP-/NLS) induced reduction of the fast and increase in the slow population is similar to that produced by at-RA but less pronounced. I-immobile (nonrecovering) RXR-YFP; M–mobile (recovering) RXR-YFP. b: FRAP mobility of FGFR1-EGFP is affected by at-RA in live cells. NB cells were transiently transfected with FGFR1-EGFP. Twenty-four hours after the transfection cells were treated with or without 1 μM at-RA for an additional 24 h. Images show an example of FGFR1-EGFP-expressing cell before and after photobleaching. FGFR1-EGFP is expressed in the cytoplasm and nucleus. Like previously we obtained a better fit using a bimodal analyses of the FGFR1-EGFP recovery curves ($R^2 = 0.992$) rather than a single exponential model ($R^2 = 0.704$). The mobile nuclear FGFR1-EGFP consists of hyperdynamic (fast "f") and hypodynamic (slow "s") populations. The immobile population shows no recovery within 3 min after bleaching. Two-exponential analysis of FGFR1-EGFP FRAP recovery ($n > 18$) shows that at-RA increases the total mobile population by increasing the slow population. The rate of slow populations displays a reduction (increased $t_{1/2}$), however, this trend did not attain statistical significance ($P = 0.089$). The effects of at-RA on FGFR1-EGFP mimics those observed during nuclear FGFR1-dependent transcriptional activation by cAMP[Dunham-Ems et al., 2009]. I -immobile (nonrecovering) FGFR1-EFP; M—mobile (recovering) FGFR1-YFP

Fig. 3. (*Overleaf*) Interaction of FGFR1 with retinoid receptors. a: at-RA treated (48 h) differentiating mESC were co-immunostained with monoclonal αFGFR1 (+ goat-anti-mouse Alexa488) and rabbit αRAR or αRXR (+ goat-anti rabbit Alexa 568). Examples of confocal sections through the middle of the nuclei are shown. In the right column only the colocalized pixels are shown in white. Colocalized FGFR1 and RAR (top row) or RXR (bottom row) IR pixels are concentrated in both the cytoplasm and nucleus. Bar size = 20 μm. b: Co-immunoprecipitation of FGFR1 with RAR and RXR. mESC were incubated for 48 h with or without (control) 1 μM at-RA. Antibody pull down was performed with αFGFR1 (C-terminal, Santa Cruz), αRXR, αRAR, or control IgG and the proteins were immunoblotted with N-terminal αFGFR1 McAb6. Interaction between FGFR1 and RXR or RAR is observed in the nucleus (top) and cytoplasm (middle) in both control and at-RA treated mESC. Following at-RA treatment there is an apparent increase in FGFR1-RAR association in the nucleus and a reduced association in the cytoplasm. These apparent changes may reflect the up-regulation of FGFR1 in the nucleus and down-regulation in the cytoplasm illustrated in the direct western blot of the isolated fractions (bottom) which is consistent with Figure 1b. However, due to the semi-quantitative nature of the co-IP assay these changes were not further considered. The equal loading in the direct western was verified by immunoblotting with anti-GDPH a predominantly cytoplasmic protein which is also present in the cell nucleus [Sen et al., 2008; Kornberg et al., 2010]. These results confirm nuclear accumulation of FGFR1 in separate experiments normalized to Ponceau S Red (Fig. 1b) or αMatrin (Fig. 3a; S1A). c: Reverse co-immunoprecipitation of RAR and RXR with FGFR1 from mESC (b). Antibody pull down was performed with αFGFR1 (C-terminal, Santa Cruz), αRXR, αRAR, or control IgG and the proteins were immunoblotted with αRAR (top) or αRXR (bottom). Interaction of RXR and RAR with FGFR1 is observed in cytoplasmic and nuclear fractions. d: Human NB cells were treated with at-RA for 0, 2, 4, or 24 h. (Top) Nuclear proteins were immunoblotted with αFGFR1 (McAb6), RAR Ab, or αMatrin (nuclear matrix associated protein, loading control). at-RA produces a gradual increase in nuclear FGFR1 and RAR contents. (Bottom—co-immunoprecipitation of FGFR1 with αRAR and αCBP shows an interaction between endogenous FGFR1 and RAR and confirms the FGFR1 interaction with CBP [Fang et al., 2005]. e: Human NB cells were co-transfected with plasmids expressing FGFR1, RXR, and RAR. Nuclear proteins were pulled down with αFGFR1 (C-terminal, Santa Cruz), αRXR, αRAR, or control IgG and immunoblotted with αFGFR1 (McAb6). A strong FGFR1 signal is observed with the αRXR and αFGFR1 pull down and a weaker signal with the αRAR pull down. f: Reverse co-IP of nuclear RAR with αFGFR1 and co-IP with αRXR and αRAR. The same nuclear extracts as in (e) were used. Pulled-down proteins were immunoblotted with αRAR. g: Reverse co-IP of RXR with αFGFR: NB cells were transfected with FGFR1, RXR, and RAR. Cytoplasmic and nuclear proteins were pulled down with αFGFR1 (C-terminal Santa Cruz), αRXR or control IgG and immunoblotted with αRXR. h: HEK cells were transfected with plasmids expressing FGFR1 or control B-gal. A robust expression of transfected FGFR1 is observed in the cytoplasmic and nuclear fractions. Endogenous FGFR1 (B-gal transfection) in HEK cells is below detection levels by direct immunoblotting. i: Co-immunoprecipitation assay. HEK cells were co-transfected with FGFR1-Flag and RXR or control B-gal. Pull down was performed with αFlag, αRXR, and IgG mouse (IgGm) or IgG Rabbit (IgGr) and immunoblotted with αFlag. A strong Flag signal is observed in the input proteins from the FGFR1-Flag and RXR transfection, while no signal is observed in B-gal input. αRXR pull down shows a Flag signal in both the nuclear and cytoplasmic fraction. j: Co-immunoprecipitation assay. HEK Cells were transfected with B-gal, FGFR1-Flag and RXR, or RXR-Flag and FGFR1. Pull down was performed with αFlag, αFGFR1, IgGm, or IgGr and immunoblotted with αRXR (left) or αFlag (right). An RXR signal is observed in the αFlag pull down of the FGFR1-Flag + RXR transfection and no signal is observed in the B-gal transfection (left). A Flag signal is observed in the FGFR1 pull down of the RXR-Flag and FGFR1 transfection (right).

diffusing protein (same as the non-fused EGFP), (ii) a slower mobile (T1/2 = 20–100 s) which reflects FGFR1 binding to nuclear protein CBP and chromatin, and (iii) an immobile (non-recovering) nuclear matrix associated FGFR1 population (Note 3 in supplementary material). In the present study, as previously found [Dunham-Ems et al., 2009], the FGFR1-EGFP FRAP curves (Fig. 4b) had a better fit to a two-exponential model ($R^2 = 0.992$) rather than a single exponential model ($R^2 = 0.704$), thus confirming the two mobile (fast and slow) nuclear FGFR1-EGFP populations (Fig. 4b).

At-RA treatment alters the overall shape of the FRAP curves, decreasing the immobile FGFR1–EGFP population by 25% and increasing the slow population nearly threefold (Fig. 4b). Thus, stimulation of retinoid receptors promotes nuclear complexes that exhibit reduced FGFR1–EGFP mobility. We conclude that the nuclear mobility of RXR and FGFR1 in live cells is reduced by conditions that promote mutual interactions. The pattern of these changes, similar to those during cAMP stimulation [Dunham-Ems et al., 2009], suggests increased involvement of FGFR1 and RXR in chromatin binding and gene transcription.

### FGFR1 INTERACTION Nur77 AND Nurr1

Developmental functions of RXR are executed in part by dimerization with closely related orphan receptor Nur77 and also Nurr1 [Watson and Milbrandt, 1990; Woronicz et al., 1994; Zetterstrom et al., 1997; Castillo et al., 1998; Saucedo-Cardenas et al., 1998; Backman et al., 1999; Kolluri et al., 2003]. Confocal microscopy reveals co-localization of FGFR1-IR with proteins recognized by pan-αNur77/Nurr1 (Fig. 5a). To further determine whether FGFR1 interacts with Nur77 and Nurr1 we carried out a series of co-immunoprecipitation experiments. In NB cells endogenous nuclear FGFR1 is immunoprecipitated by αRXR as well as αNurr77/Nurr1 (Fig. 5b). Co-transfection of FGFR1 with Nurr1 and RXR markedly increases the amount of FGFR1 precipitated by αFGFR1, αRXR, and αNurr77/1. Figure 5b also shows the reverse immunoprecipitation of endogenous and transfected Nurr1 with αRXR and αFGFR1. The interaction between FGFR1 and Nurr1 was further established in HEK cells in which transfected Nurr1-Flag is co-precipitated with αFGFR1 and detected using αFlag (Fig. S3). Additionally, FGFR1 co-precipitates with Nur77 based on a Nur77 selective antibody. Finally, GST-RAR, but not GST, pulls down Nur77 as well as the hypo-and hyper-glycosylated forms of nuclear FGFR1-Flag (Fig. 5c).

### FGFR1 ASSOCIATION WITH NUCLEAR TRANSCRIPTION SITES AND at-RA-ACTIVATED GENES IN mESC

FGFR1 is concentrated in nuclear speckles that contain RNA Polymerase II, splicing factors, and acetylated and phosphorylated histones [Peng et al., 2002; Somanathan et al., 2003]. Approximately 40% of the total FGFR1-IR co-localizes with transcriptionally active sites while less than 4% overlap with DNA replication sites [Somanathan et al., 2003]. In mESC, the 5′Fluoro-Uridine (FU)-labeled transcription sites are concentrated in the nucleoli and discrete FGFR1/RXR-rich extra-nucleolar domains (Fig. S4A). Fractions of co-localized extranucleolar pixels were estimated as Manders' Coefficients (M); $0.439 \pm 0.0225$ of FGFR1-IR pixels overlap with RXR-IR pixels and $0.564 \pm 0.025$ of RXR-IR pixels overlap with FGFR1-IR pixels. Co-localization of FGFR1-IR with FU-IR is $M = 0.407 \pm 0.024$ and colocalization of RXR-IR

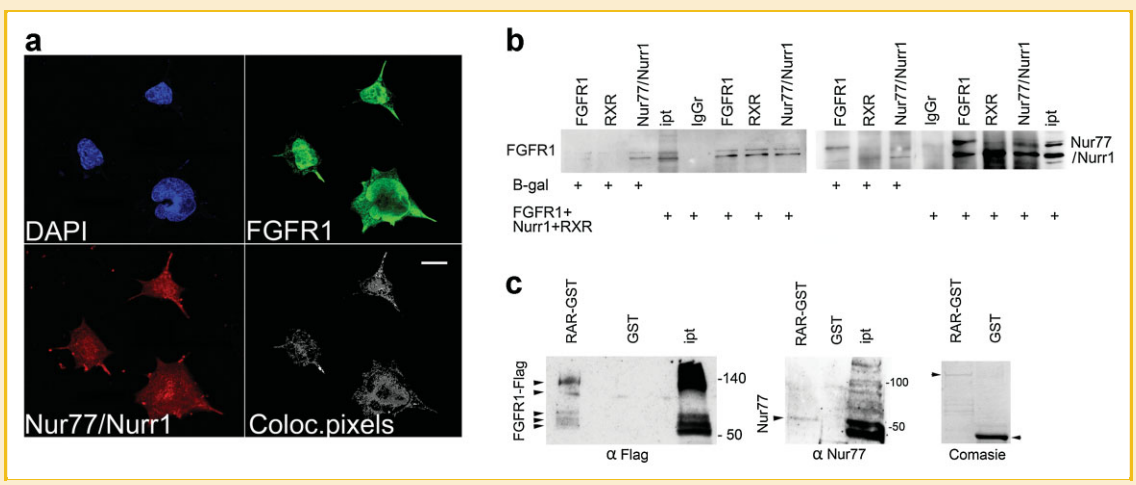


Fig. 5. Interaction of FGFR1 and Nur proteins. a: Concentrations of colocalized FGFR1 and Nur77/Nurr1 IR pixels are observed in both the cytoplasm and the nucleus. at-RA treated (48 h) differentiating mESC were co-immunolabeled with mouse monoclonal αFGFR1 (ABCAM) (+ goat-anti-mouse Alexa 488, green) and rabbit αNur77/Nurr1 (+ goat-anti-rabbit Alexa 568, red). Examples of confocal sections through the middle of the nuclei are shown. In the right column only the colocalized pixels are shown in white. Concentrations of colocalized FGFR1 and RAR IR pixels (top row) and FGFR1 and RXR IR pixels (bottom row) are observed in both the cytoplasm and nucleus. Bar size = 20 μm. b: Co-immunoprecipitation assay. Neuroblastoma (NB) cells were transfected with B-gal or FGFR1 with Nurr1 and RXR. Endogenous FGFR1 is co-immunoprecipitated by αNur77/Nurr1 and immunoblotted with αFGFR1 (left). Stronger FGFR1 signals are observed in cells co-transfected with FGFR1, Nurr1, and RXR. Endogenous Nur77/Nurr1 is co-immunoprecipitated with αFGFR1 and αRXR and immunoblotted with αFGFR1 (right). A strong Nur77/Nurr1 signal is observed with αFGFR1 and αRXR pull down in FGFR1, Nurr1, and RXR transfection. c: Affinity selection of FGFR1 and Nur77 by GST-RAR. GST or GST-RAR fusion [Qiu et al., 2007] proteins were expressed in *E.Coli* and used to isolate nuclear proteins from NB cells transfected with FGFR1-Flag (A) and Nur77. The GST-selection of nuclear extracts was followed by western blotting with αFlag (left) or αNur77/Nurr1 (middle). GST and GST-RAR were detected by direct gel staining with Coommasie Blue (right).

with FU-IR is $M = 0.463 \pm 0.026$. Importantly, the overlap with FU-IR is significantly greater for co-localized FGFR1-IR and RXR-IR than for RXR-IR or FGFR1-IR, which are not co-localized (Fig. S4B). Thus, the probability of active transcription increases in sites co-inhabited by both RXR and FGFR1.

Nuclear accumulation of FGFR1 in mESC also coincides with histone H3 lysine-dimethylation (Fig. S4C,D), which marks transcriptionally active chromatin, and with histone H3.3, which replaces histone H3 in transcriptional poised chromatin (Fig. S4E).

### INTERACTION OF FGFR1 WITH AT-RA ACTIVATED GENES IN mESC

Gene array studies have identified a number of genes in mESC which are up-regulated by at-RA accompanying differentiation [Guan et al., 2001]. Figure 6a shows the upregulation of *fgfr1, fgf-2*, and *th* mRNA in the presence of at-RA. Since these genes are also activated by nuclear FGFR1 [Peng et al., 2001; Peng et al., 2002; Fang et al., 2005], we performed ChIP in order to identify the presence of FGFR1 on regulatory regions related to the canonical NR motif AGGTCA known to bind Nur, RXR, and RAR proteins. Our previous studies demonstrated FGFR1 binding to the *fgf-2* gene promoter and a lack of binding to the glyceraldehyde-3-phosphate dehydrogenase (GADPH) [Fang et al., 2005]. Here we identified AGGTCA-containing potential regulatory elements for Nur77/Nurr1 in the distal and proximal promoter region of the *fgf-2* and *fgfr1* genes, respectively. Each region is effectively immunoprecipitated with αFGFR1 and αNur77/Nurr1 and treatment with at-RA increases protein binding to the promoter (Fig. 6b,c). Expression of the *th* gene during development is critically dependent on the Nurr1 protein [Smidt and Burbach, 2009]. We identified a target site for Nur77/Nurr1 in the mouse *th* gene (GTTCTC-4x-GTTCAC) which binds FGFR1 and Nur77/Nurr1 and is enhanced in the presence at-RA (Fig. 6d). DNA bound FGFR1 and Nur77/1 is also associated with the FGFR1 transcriptional partner CBP and up-regulated by at-RA (Fig. 6b–d). Additionally, we observed an at-RA-induced incorporation of H3.3, which is either delayed compared to Nur (*fgf-2* gene, Fig. 6b), or follows similar biphasic changes (decrease at 3 h followed by an increase at 6 h; *fgfr1* and *th* genes, Fig. 6c,d). These observations indicate dynamic changes in Nur and FGFR1 binding and associated chromatin remodeling at the sites of neurogenic (*fgfr1, fgf-2*) and neuronal (*th*) genes. Consistent with an earlier report that the *Prm*1 gene is not stimulated by at-RA in mESC [Guan et al., 2001] we observed no changes in FGFR1 and Nur binding to the *Prm1* gene promoter (not shown).

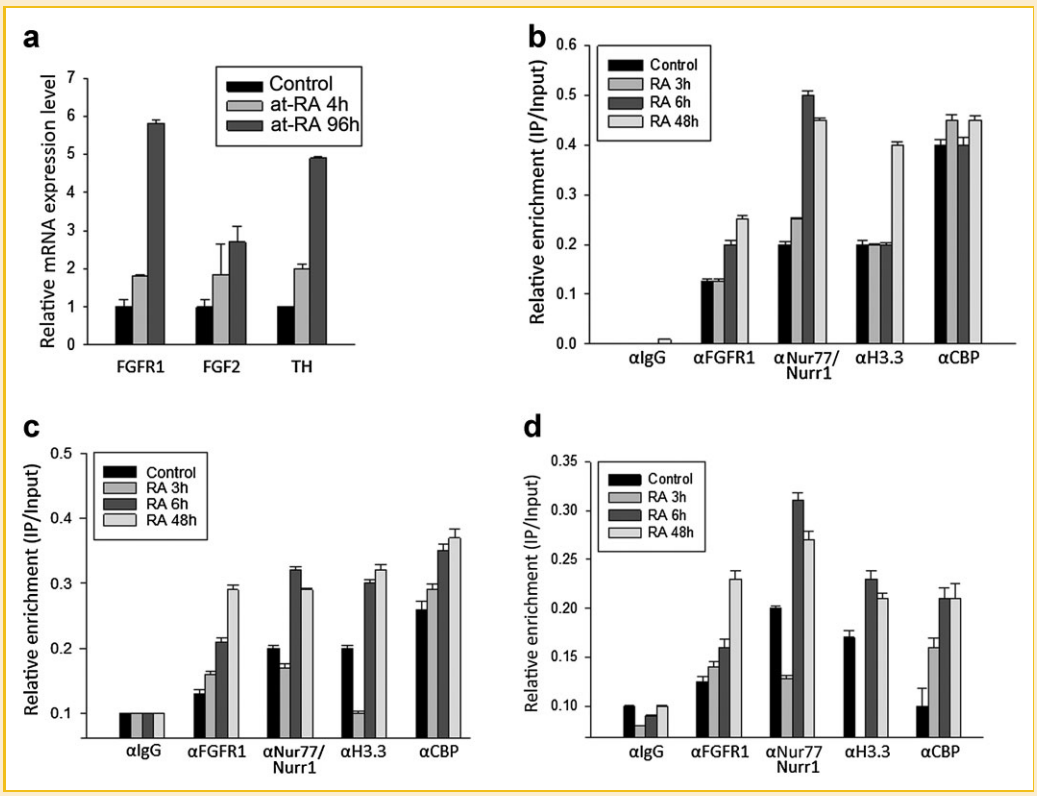


Fig. 6. at-RA induced gene activation in mESC and in vivo FGFR1 binding to activated genes. a: mESC were incubated with 1 μM at-RA for indicated periods of time. mRNA levels of *fgfr1*, *fgf-2*, and *th* in control and at-RA treated cells were measured by RTqPCR. Gene expression was quantified as described [Pfaffl, 2001]. b–d):Chromatin immunoprecipitation (ChIP) was performed with a panel of antibodies against FGFR1, Nur77/1, CBP, and histone H3.3 with subsequent qPCR analyses of selected potential RXR/Nurr1 binding regions on (b) *fgf-2* (c) *fgfr1* and (d) *th* genes. IgG was used as a negative control. Graphs show mean ± SEM of triplicate samples from one of two separate experiments.

## CO-ACTIVATION OF TRANSCRIPTION BY FGFR1, NURS, AND RETINOID RECEPTORS

We next determined whether increased FGFR1 and Nur77/Nurr1 binding to the NR core sites affect transcription. Monomeric Nur77 and Nurr1 activate transcription by binding to the canonical NR motif AGGTCA present in the NBRE target sequence [Maira et al., 1999]. Figure 7a shows Nur77 activates NBRE approximately sixfold. Cotransfected nuclear FGFR1(SP-/NLS) potentiates this activation nearly three times to 17-fold. Nur77 NBRE-dependent activation is also augmented by the 23 kDa form of FGF-2 (Fig. S5), which binds and activates endogenous nuclear FGFR1 [Peng et al., 2002; Dunham-Ems et al., 2009]. The 18 kDa FGF-2, which does not interact with nuclear FGFR1, has no effect on Nur77 NBRE-dependent transcription.

The Nur-response element (NurRE), a transcriptional target site for Nur homo/heterodimers [Maira et al., 1999, 2003], is comprised of an octameric everted repeat related to the NBRE. Nur77 markedly enhances NurRE-dependent transcription in both NB and HEK cells. In NB cells, Nur77-dependent transcription of the NurRE is synergistically enhanced by nuclear FGFR1(SP-/NLS) and reduced by dominant negative FGFR1 (TK-) (Fig. 7b). In addition, we compared the effects of nuclear FGFR1 on Nur77 and Nurr1 NurRE activation. In HEK cells, nuclear FGFR1(SP-/NLS) has a more pronounced effect on NurRE activation by Nur77 than by Nurr1 (Fig. S6A,B). Transcription activation by Nur77 and its augmentation by FGFR1(SP-/NLS) (Fig. 7a) or 23 kDa FGF-2 (Fig. S5) are not observed on the minimal POMC promoter which lacks Nur binding sites. Together, these experiments reveal synergistic activation of NBRE and NurRE-dependent transcription by orphan Nur77 receptors and nuclear FGFR1.

Nur77 and Nurr1 can also heterodimerize with RXR, a common and versatile NR partner, and mediate retinoid-dependent transcription by acting on RAREs comprised of the canonical NR motif AGGTCA separated by 5-base pairs (DR5). RARE can act in isolation from other cis-elements to confer retinoid stimulation. Hence, functions of RAR stimulated by at-RA and 9cis-RA, or RXR stimulated by 9cis-RA, can be effectively assessed using promoter systems containing only this element. In NB cells we used a construct containing eight copies of the RARE (DR5) upstream from the TATA box [Hoffman et al., 2006]. First, to determine if FGFR1 and RXR directly target RAREs we performed ChIP analysis (Fig. 8a). Overexpressed FGFR1-Flag and RXR-Flag both bind the RARE-reporter but only RXR binding increases in the presence of at-RA.

Stimulation of an RARE-luc reporter by at-RA is observed at a concentration of 1 nM and is increased further with higher concentrations of at-RA (Fig. S7). Figure 8b shows a sevenfold activation of RARE-luc by 1 μM at-RA which is significantly enhanced by constitutively active nuclear FGFR1(SP-/NLS). In contrast, at-RA activation is reduced to twofold by co-transfected FGFR1(TK-) and fivefold by FGFR1(SP-/NLS)(TK-) (Fig. 8b). The smaller effect of FGFR1(SP-/NLS)(TK-) may reflect its lower expression levels. Expression levels of FGFR1(SP-/NLS) or FGFR1(SP-/NLS)(TK-) are typically similar to endogenous FGFR1 while FGFR1(TK-) is expressed at a 2–3-fold higher level (not shown) [Peng et al., 2001; Dunham-Ems et al., 2009].

In HEK cells, which contain low amounts of endogenous RXR and FGFR1, the effect of FGFR1(SP-/NLS) on at-RA stimulation is more pronounced than in NB cells but requires co-transfected RXR. The overexpression of RXR has no effect on at-RA mediated transcription, consistent with the known inability of at-RA to activate RXR.

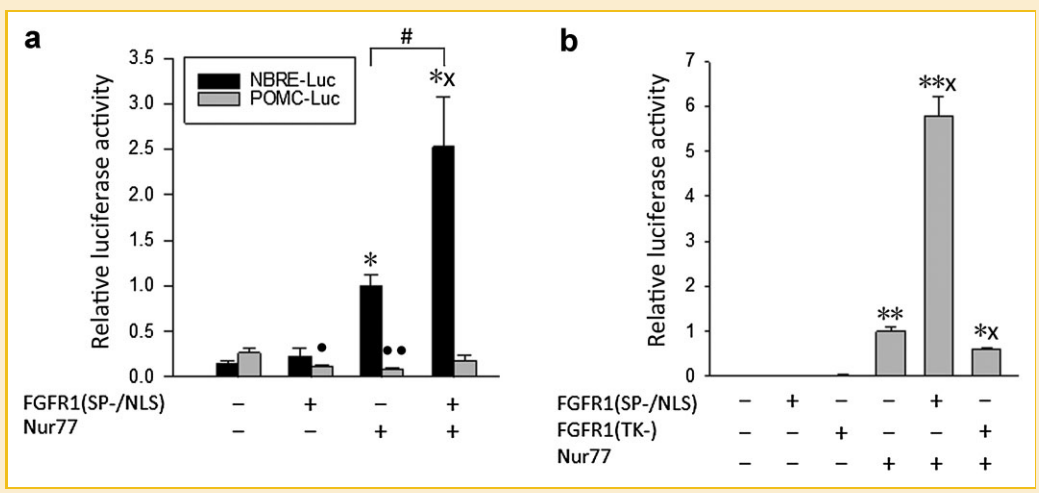


Fig. 7. FGFR1 augmentation of Nur77-dependent transcription on the NBRE or NurRE in NB cells. a: The NBRE reporter or the minimal POMC promoter (TATA box, deleted Nur elements) was cotransfected with nuclear FGFR1(SP-/NLS) in the presence or absence of Nur77. The total amount of transfected DNA per well was adjusted to 1 μg by addition of B-gal plasmid. Results are shown as the mean ± SEM. FGFR1(SP/NLS) enhances Nur77-dependent transcription of the NBRE reporter. The minimal POMC promoter showed no stimulation by Nur77 or FGFR1(SP-/NLS). NBRE-1wANOVA $^{\#}P > 0.001$ significance between Nur77 and FGFR1(SP-/NLS), $^{*}P \geq 0.001$ difference to β-gal. 2wANOVA: Nur77 and FGFR1(SP-/NLS) overall effect-$P > 0.001$; (x) Interaction-Nur77 x FGFR1(SP-/NLS) $P = 0.001$. POMC-1wANOVA: Significant decrease •$P > 0.05$, ••$\geq 0.001$. b: Cells were transfected with the NurRE reporter and either FGFR1(SP-/NLS) or dominant negative FGFR1(TK-) in the presence or absence of Nur77. The transcriptional activity of Nur77 on the NurRE reporter, which binds and is activated by Nur dimers, is strongly enhanced by nuclear FGFR1(SP-/NLS) while FGFR1(TK-) represses activation. FGFR1(SP-/NLS) or FGFR1(TK-) has no effect on the NurRE in the absence of Nur77. 1wANOVA:$^{**}$ $P > 0.001$, $^{*}P > 0.05$ difference to β-gal. .2wayANOVA: Nur77 and FGFR1(SP-/NLS) overall effect-$P > 0.001$, FGFR1(TK-) overall effect-$P > 0.005$; (X) Interaction-Nur77 x FGFR1(SP-/NLS) $P > 0.001$, Nur77 x FGFR1(TK-) $P > 0.005$.

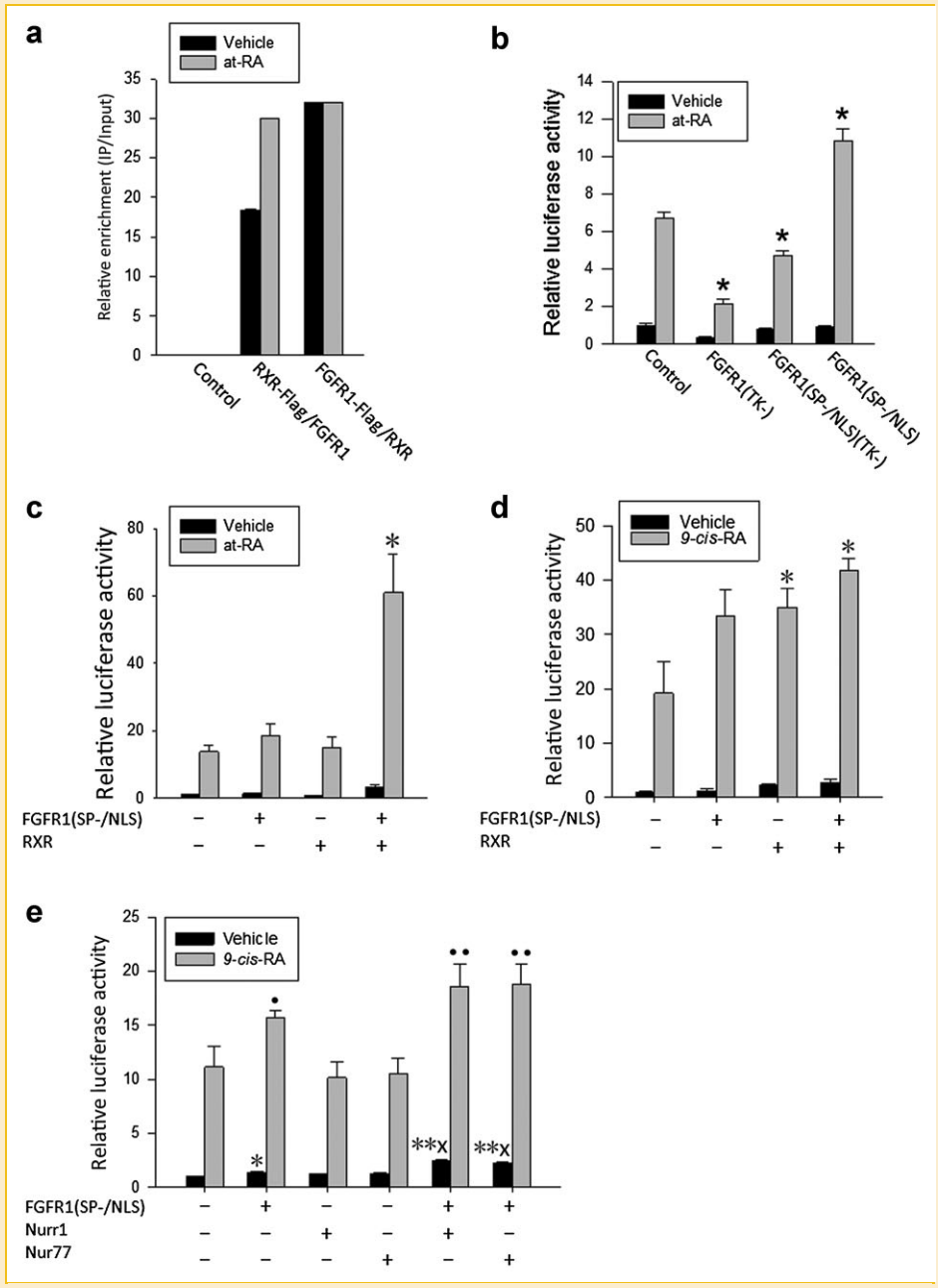


Fig. 8. FGFR1 augmentation of RARE-dependent transcription. a: ChIP assay. NB cells were transfected with control B-Gal, RXR-Flag/FGFR1, or FGFR1-Flag/RXR plasmid along with RARE-Luc and Renilla. Chromatin was immunoprecipitated with αFGFR1, αFlag, or control IgG. Immunoprecipitated and input DNA were analyzed using primers which encompass the 8XRARE promoter region. Plasmids expressing FGFR1 and RXR bind to the RARE sequence whereas control B-Gal plasmid does not. b: Nuclear FGFR1 affects transcriptional activation by at-RA. NB cells were transfected with RARE-Luc, and with control pcDNA3.1(−) or pcDNA3.1 expressing an active nuclear FGFR1(SP-/NLS), dominant negative FGFR1(SP-/NLS)(TK-) (exclusively nuclear protein) or FGFR1(TK-) (cytoplasmic and nuclear protein). Thirty-six hours after transfection cells were treated for an additional 24 h with 1 μM at-RA or 0.001% DMSO (control). Nuclear FGFR1(SP-/NLS) increases at-RA stimulation from 6-fold to 11-fold while FGFR1(TK-) and FGFR1(SP-/NLS)(TK-) significantly decrease at-RA stimulation. Two-way ANOVA demonstrates a statistically significant interaction between all transfected FGFR1 constructs and RA stimulation ($P > 0.01$).$^{*}P > 0.001$ different from pcDNA3.1 control. Transfected FGFR1 proteins have no significant (NS) effect on basal promoter activity. c: Synergistic activation of transcription by RXR and nuclear FGFR1. HEK cells were transfected with the RARE-Luc reporter, FGFR1(SP-/NLS), RXR, or both RXRα and FGFR1(SP-/NLS). The total amount of transfected DNA per well was adjusted to 1 μg with pcDNA3.1(−). Forty-two hours after transfection cells were treated with at-RA for an additional 24 h and harvested for dual luciferase reporter assay. Results are shown as the mean ± SEM. Neither RXR nor FGFR1(SP-/NLS) alone have an effect on basal or at-RA induced RARE promoter activity. Together, FGFR1(SP-/NLS) and RXR augment the RA stimulation from 18-fold to approximately 60-fold.$^{*}P = 0.001$ different from pcDNA3.1. d: Nuclear FGFR1(SP-/NLS) does not augment 9c-RA mediated activation of the RARE. In HEK cells FGFR1(SP-/NLS) augmentation of RARE-dependent transcription was assessed by cotransfection of the RARE-Luc, RXRα or nuclear FGFR1(SP-/NLS), or RXRα and FGFR1(SP-/NLS). The total amount of transfected DNA per well was adjusted to 1 μg with B-gal. Thirty-six hours after transfection cells were treated with 1 μM 9c-RA for an additional 24 h and harvested for the reporter assay. Results are shown as the mean ± SEM. Statistics—basal activity: 1wANOVA: $^{*}P > 0.05$, $^{**}P > 0.005$ difference from β-gal. 2wANOVA: RXR overall effect $P > 0.005$, No RXR+ FGFR1(SP-/NLS) interaction. 9c-RA activation: 1wANOVA:•$P > 0.05$, ••$P > 0.01$ difference to β-gal. 2wANOVA: FGFR1(SP-/NLS) and RXR overall effect-$P > 0.05$, no RXR+ FGFR1(SP-/NLS) interaction. e: Nuclear FGFR1 enhancement of Nurr1 and Nur77 RARE-dependent transcription in the presence and absence of 9c-RA. HEK cells were transfected with the RARE-Luc and Nurr1 or Nur77 in the presence or absence of FGFR1(SP-/NLS). The total amount of transfected DNA per well was adjusted to 1 μg by addition of B-gal. Thirty-six hours after transfection cells were treated with 1 μM 9c-RA for an additional 24 h and harvested for the reporter assay. Results are shown as the mean ± SEM. Basal promoter activity: 1wANOVA:$^{*}P > 0.01$, $^{**}P > 0.001$ difference from B-gal. 2wANOVA: FGFR1(SP-/NLS), Nurr1, and Nurr77 overall effect-$P > 0.001$. (X) interaction-FGFR1(SP-/NLS)xNurr1 $P > 0.001$, NLSxNur77-$P > 0.005$. 9c-RA stimulation: 1wANOVA: •$P > 0.05$, ••$P > 0.005$ difference from β-gal. 2wANOVA: FGFR1(SP-/NLS)overall effect $P > 0.001$ while Nurr1 or 77 have no effect, no FGFR1(SP-/NLS) + Nurr1/77 interaction.

Also, FGFR1(SP-/NLS) alone has no effect on transcription, however, when overexpressed together with RXR activation increases markedly from 18-fold to over 60-fold (Fig. 8c). Thus, FGFR1 (SP-/NLS) synergistically enhances RARE-mediated transcription by influencing the activity of RXR in the presence of an RAR ligand, at-RA. This synergistic effect of FGFR1 and RXR does not occur in the presence of 9c-RA when both RXR and RAR are activated (Fig. 8d). Hence, the ability of FGFR1 to function as an RA-dependent transcriptional regulator is limited to at-RA.

Nur77 and Nurr1 also form retinoid permissive heterodimers with RXR and activate transcription by binding DR5 target sequences. Consistent with a previous report [Maira et al., 1999] we observe no effect of Nur77 or Nurr1 on basal RARE-luc activity (Fig. 8e). However, when co-transfected with FGFR1(SP-/NLS) the basal RARE activity increases synergistically threefold, further indicating a functional partnership between Nur77/Nurr1 and nuclear FGFR1 on RARE-dependent gene activation. Nuclear FGFR1 potentiates the transcriptional activity of Nur77 and Nurr1 on the RARE in the absence and presence of 9c-RA, however, FGFR1 enhancement of 9c-RA transcriptional activation is not augmented upon the addition of either Nur factor (Fig. 8e). Collectively, these experiments indicate two primary functions of nuclear FGFR1 in RARE-mediated gene expression: (1) Augmentation of at-RA stimulation by enhancing the transcriptional activity of unliganded RXR and (2) increasing the basal transcriptional activity of Nur77 and Nurr1 in the absence of a ligand.

## DISCUSSION

Integrative Nuclear FGF Receptor-1 (FGFR1) Signaling (INFS) mediates gene activation at different chromosomal loci associated with postmitotic development and neuronal-like differentiation. In INFS activation, FGFR1, a membrane-targeted protein, translocates to the nucleus and further executes the release and subsequent activation of CBP, a transcriptional co-activator that is the ''End Gate'' of numerous signaling transduction pathways. We demonstrate that nuclear FGFR1 also mediates the transcriptional activity of other NR subfamilies that regulate neuronal gene expression through differential mechanisms not associated with ''classical'' signaling cascades. Prior to the current work, it was unknown whether this distinctive category of directly acting, nuclear developmental transducers, such as the dual function retinoid receptors, may also utilize and/or is influenced by the INFS mechanism. The results show that nuclear FGFR1 interacts with and augments the transcriptional function of RAR/RXR and orphan Nur receptors on target binding motifs related to, or containing the canonical, RARE, NBRE, or NurRE during RA-mediated neuronal differentiation of mESC. These results support our recent finding that in rodent brain dopamine neurons FGFR1 colocalizes and interacts with Nurr1 and coactivates TH gene promoter elements [Baron et al., 2012].

A central and essential functional feature of the INFS, RAR, RXR, and Nur modules is the nuclear accumulation of FGFR1, which constitutes a common developmental response to at-RA in pluripotent mouse and human ESC and multipotent NPC. at-RA affects FGFR1 biology by increasing levels of FGFR1 mRNA as well as shifting FGFR1 protein from the cytoplasm to the nucleus as evidenced by the depletion of cytoplasmic FGFR1 and an increase in nuclear FGFR1 content. The nuclear accumulation of FGFR1 was previously shown to be mediated by importin-β which binds the Nuclear Localization Sequence (NLS) [Reilly and Maher, 2001]. The present studies indicate that FGFR1, which lacks NLS, could be chaperoned by an NLS-equipped 23 kDa FGF-2 as well as RAR/RXR, which interact with FGFR1 both in the cytosol and nucleus and promote FGFR1 nuclear accumulation.

The functional importance of nuclear FGFR1 accumulation during mESC differentiation was elucidated through our experimental design using a recombinant FGFR1(SP-/NLS) construct in which the signal peptide is replaced with NLS. FGFR1(SP-/NLS), which is targeted to the nucleus without an NLS-providing chaperone and without initial synthesis as an ER membrane inserted protein, allowed us to establish a causal relationship between at-RA-induced mESC differentiation and nuclear accumulation of FGFR1. The importance of endogenous nuclear FGFR1 transfer is underscored by the observation that dominant negative FGFR1(SP-/NLS)(TK-) prevents at-RA induced neurite outgrowth. Furthermore, transfection of the tyrosine kinase-containing nuclear FGFR1(SP-/NLS) was sufficient to promote neuronal-like differentiation in the absence of at-RA. The extent of this differentiation will be investigated further to delineate the expression of neuronal proteins and associated physiological features [Sun et al., 2005]. Thus far, activation of INFS by transfection of nuclear FGFR1 or 23 kDa FGF-2 induces an exit from the cell cycle, morphological differentiation and the expression of neuron-specific proteins in human brain [Stachowiak et al., 2003a]-or umbilical cord blood [Fang et al., 2005]-derived Neural Progenitor Cells, neoplastic pheochromocytoma, medulloblastoma and neuroblastoma cells [Stachowiak et al., 2003a; Fang et al., 2005; Stachowiak et al., 2009] and the reinstatement of neuronogenesis in the adult brain in vivo [Bharali et al., 2005; Stachowiak et al., 2009].

A central finding of our investigation is the association of FGFR1 with retinoid and orphan Nur NRs. The interaction between endogenous and transfected recombinant proteins was shown by bidirectional co-IP assays with antibodies against FGFR1, RAR, RXR, and Nurs and further verified using flag-tagged proteins and GST-affinity selection. Confocal microscopy places FGFR1 interactions with RAR/RXR and Nurs at multiple cell compartments: Cytoplasm, nuclear membrane, and nuclear interior. Within the nucleus, FGFR1 staining co-localizes predominantly with weak DAPI staining, indicating a preferential association with euchromatin and an exclusion from heterochromatin. This is further supported by FGFR1 co-localization with the tri-methylated histone H3K4 and replacement with the H3.3 variant, which marks transcriptionally poised active chromatin [Goldberg et al., 2010; Shahhoseini et al., 2010].

FRAP analysis reveals a reduction in the nuclear mobility of RXR and FGFR1 by conditions that promote their mutual interaction, supporting the formation of nuclear FGFR1-RXR complexes in live cells. Similarly, a reduction in FGFR1 mobility by overexpressed Nurr1 recently observed in our additional studies (Note 4 in supplementary material) further support the FGFR1-Nurr1 interactions.

These interactions and co-localizations of FGFR1 with classical NRs further establish the role of FGFR1 as an integrative nuclear signaling factor. Whether FGFR1 binds with RXR, RAR, and Nurs directly or via common partner proteins, such as CBP, must be addressed in future studies to further understand these interactions.

Several observations indicate the roles for FGFR1 modules with RAR/RXR and Nur77/Nurr1 in gene activation. FGFR1-mediated gene activation correlates with the conversion of immobile matrix-bound and fast nuclear FGFR1 into a slow chromatin binding population [Dunham-Ems et al., 2009]. By increasing the residence time of FGFR1 and its partner proteins the transcriptional reaction may be initiated and carried to the completion of RNA transcripts, similar as proposed in the oscillatory model of RNA Polymerase II [Darzacq et al., 2007]. The pattern of RA-induced changes in nuclear FGFR1 mobility and FGFR1-induced changes in RXR mobility is consistent with the oscillatory model and further suggests an involvement of FGFR1 and RXR in chromatin binding and gene transcription. In agreement with the kinetic changes observed, the steady-state concentration of FGFR1 and its partners in transcriptionally active domains is accompanied by suitable epigenetic histone modifications. FGFR1 co-localizes with FU-labeled nuclear sites of RNA synthesis and the probability of active transcription increases in sites co-inhabited by both RXR and FGFR1. The indicated function of FGFR1 as a global gene activator may be endowed by interactions with RAR/RXR, Nur77 (present study) and common transcription co-activators (CBP) [Fang et al., 2005]. Furthermore, the overall nuclear accumulation of FGFR1 coincides with tri-methylated histone H3K4, which marks transcriptionally active chromatin, and with histone H3.3, which replaces histone H3 in transcriptionally poised chromatin.

The gene activating function of FGFR1 modules are further elucidated by the association of FGFR1 and Nur77 on at-RA-activated neurogenic (*fgf-2, fgfr1*) and neuronal (*th*) genes, previously shown to be activated by nuclear FGFR1 [Peng et al., 2001; Peng et al., 2002]. As shown in the present study, FGFR1 interacts with DNA elements containing consensus sequences for RXR and Nur and FGFR1/Nur binding is enhanced by at-RA. The dynamic changes in Nur and FGFR1 binding are also accompanied by the transcriptional co-activator CBP and the incorporation of H3.3, indicative of chromatin remodeling.

The roles of FGFR1-RAR/RXR and FGFR1-Nur regulatory modules in gene activation were illustrated by reporter assays employing isolated RARE, NBRE, and NurRE response elements. These experiments show that FGFR1 works together with RAR/RXR during the transduction of at-RA stimulation and augments the ligand-independent function of RXR and Nur. In addition, INFS activation provides a mechanism sufficient to promote RXR and Nur-dependent gene activation in the absence of at-RA. Therefore, we propose that FGFR1 serves as an essential scaffolding co-factor for retinoid receptor- and Nur-mediated gene activation. This function may explain the ability of nuclear FGFR1 to promote neuronal programming of mESC in the absence of at-RA.

FGFR1, through the partnership with CBP, can activate gene elements (CRE, AP1, and NfkB) which do not bind retinoid or orphan NRs. Hence, whether RA-induced nuclear FGFR1 accumulation promotes genome-wide re-programing encompassing genes that are not directly regulated by RAR, RXR, or Nurs should be addressed.

In summary our investigation expands the notable integrative function of INFS so that it now includes retinoid and orphan nuclear receptors. These novel regulatory modules offer potential targets for the activation of developmental processes in pluripotent and multipotent stem cells.

## ACKNOWLEDGMENTS

The authors gratefully acknowledge the generous gift of NurRE-Luc, NBRE3-Luc, minimal POMC promoter-Luc and Nur77-expressing pCMX plasmids from Dr. Jacques Drouin (Institut de Recherches Cliniques de Montrèal). This work was supported by NYSTEM contracts C026415 and C026714 (to MKS) and C024355 (to EST). EKS was supported by NYSTEM C026714. EST was partially supported by (NIH) R21HL092398 and R01HL103709.

## REFERENCES

Backman C, Perlmann T, Wallen A, Hoffer BJ, Morales M. 1999. A selective group of dopaminergic neurons express Nurr1 in the adult mouse brain. Brain Res 851:125–132.

Baron O, Foerthmann B, Lee Y-W, Terranova C, Ratzka A, Stachowiak EK, Grothe C, Claus P, Stachowiak MK. 2012. Cooperation of nuclear FGFR1 and Nurr1 offers a new interactive mechanism in postmitotic development of mesencephalic dopaminergic neurons. J Biol Chem, DOI: 10.1074/jbc.M112.347831.

Bastien J, Rochette-Egly C. 2004. Nuclear retinoid receptors and the transcription of retinoid-target genes. Gene 328:1–16.

Berrabah W, Aumercier P, Lefebvre P, Staels B. 2011. Control of nuclear receptor activities in metabolism by post-translational modifications. FEBS Lett 585:1640–1650.

Bharali DJ, Klejbor I, Stachowiak EK, Dutta P, Roy I, Kaur N, Bergey EJ, Prasad PN, Stachowiak MK. 2005. Organically modified silica nanoparticles: A nonviral vector for in vivo gene delivery and expression in the brain. Proc Natl Acad Sci USA 102:11539–11544.

Castillo SO, Baffi JS, Palkovits M, Goldstein DS, Kopin IJ, Witta J, Magnuson MA, Nikodem VM. 1998. Dopamine biosynthesis is selectively abolished in substantia nigra/ventral tegmental area but not in hypothalamic neurons in mice with targeted disruption of the Nurr1 gene. Mol Cell Neurosci 11:36–46.

Claus P, Doring F, Gringel S, Muller-Ostermeyer F, Fuhlrott J, Kraft T, Grothe C. 2003. Differential intranuclear localization of fibroblast growth factor-2 isoforms and specific interaction with the survival of motoneuron protein. J Biol Chem 278:479–485.

Darzacq X, Shav-Tal Y, de Turris V, Brody Y, Shenoy SM, Phair RD, Singer RH. 2007. In vivo dynamics of RNA polymerase II transcription. Nat Struct Mol Biol 14:796–806.

Dong S, Stenoien DL, Qiu J, Mancini MA, Tweardy DJ. 2004. Reduced intranuclear mobility of APL fusion proteins accompanies their mislocalization and results in sequestration and decreased mobility of retinoid X receptor alpha. Mol Cell Biol 24:4465–4475.

Dunham-Ems SM, Lee YW, Stachowiak EK, Pudavar H, Claus P, Prasad PN, Stachowiak MK. 2009. Fibroblast growth factor receptor-1 (FGFR1) nuclear dynamics reveal a novel mechanism in transcription control. Mol Biol Cell 20:2401–2412.

Dunham-Ems SM, Pudavar HE, Myers JM, Maher PA, Prasad PN, Stachowiak MK. 2006. Factors controlling fibroblast growth factor receptor-1's cytoplasmic trafficking and its regulation as revealed by FRAP analysis. Mol Biol Cell 17:2223–2235.

Duong V, Rochette-Egly C. 2011. The molecular physiology of nuclear retinoic acid receptors. From health to disease. Biochim Biophys Acta 1812:1023–1031.

Elsaesser SJ, Goldberg AD, Allis CD. 2010. New functions for an old variant: No substitute for histone H3.3. Curr Opin Genet Dev 20:110–117.

Fang X, Stachowiak EK, Dunham-Ems SM, Klejbor I, Stachowiak MK. 2005. Control of CREB-binding protein signaling by nuclear fibroblast growth factor receptor-1: A novel mechanism of gene regulation. J Biol Chem 280:28451–28462.

Feige JN, Gelman L, Tudor C, Engelborghs Y, Wahli W, Desvergne B. 2005. Fluorescence imaging reveals the nuclear behavior of peroxisome proliferator-activated receptor/retinoid X receptor heterodimers in the absence and presence of ligand. J Biol Chem 280:17880–17890.

Floettmann M, Scharp T, Klipp E. 2011. Computational modeling of biochemical processes and cell differentiation. In: Stachowiak MK, Tzanakakis ES, editors. Stem cells from mechanisms to technologies E.S.T. New Jersey, London, Singapore, Beijing, Shanghai, Hong Kong, Taipei, Chennai: World Scientific Publishing. pp 3–29.

Forman BM, Umesono K, Chen J, Evans RM. 1995. Unique response pathways are established by allosteric interactions among nuclear hormone receptors. Cell 81:541–550.

Fraichard A, Chassande O, Bilbaut G, Dehay C, Savatier P, Samarut J. 1995. In vitro differentiation of embryonic stem cells into glial cells and functional neurons. J Cell Sci 108(Pt 10):3181–3188.

Germain P, Chambon P, Eichele G, Evans RM, Lazar MA, Leid M, De Lera AR, Lotan R, Mangelsdorf DJ, Gronemeyer H. 2006. International union of pharmacology. LXIII. Retinoid X receptors. Pharmacol Rev 58:760–772.

Goldberg AD, Banaszynski LA, Noh KM, Lewis PW, Elsaesser SJ, Stadler S, Dewell S, Law M, Guo X, Li X, Wen D, Chapgier A, DeKelver RC, Miller JC, Lee YL, Boydston EA, Holmes MC, Gregory PD, Greally JM, Rafii S, Yang C, Scambler PJ, Garrick D, Gibbons RJ, Higgs DR, Cristea IM, Urnov FD, Zheng D, Allis CD. 2010. Distinct factors control histone variant H3.3 localization at specific genomic regions. Cell 140:678–691.

Guan K, Chang H, Rolletschek A, Wobus AM. 2001. Embryonic stem cell-derived neurogenesis. Retinoic acid induction and lineage selection of neuronal cells. Cell Tissue Res 305:171–176.

Hanneken A, Maher PA, Baird A. 1995. High affinity immunoreactive FGF receptors in the extracellular matrix of vascular endothelial cells–implications for the modulation of FGF-2. J Cell Biol 128:1221–1228.

Hoffman LM, Garcha K, Karamboulas K, Cowan MF, Drysdale LM, Horton WA, Underhill TM. 2006. BMP action in skeletogenesis involves attenuation of retinoid signaling. J Cell Biol 174:101–113.

Horbinski C, Stachowiak MK, Higgins D, Finnegan SG. 2001. Polyethyleneimine-mediated transfection of cultured postmitotic neurons from rat sympathetic ganglia and adult human retina. BMC Neurosci 2:2.

Kehoe DE, Lock LT, Parikh A, Tzanakakis ES. 2008. Propagation of embryonic stem cells in stirred suspension without serum. Biotechnol Prog 24:1342–1352.

Kolluri SK, Bruey-Sedano N, Cao X, Lin B, Lin F, Han YH, Dawson MI, Zhang XK. 2003. Mitogenic effect of orphan receptor TR3 and its regulation by MEKK1 in lung cancer cells. Mol Cell Biol 23:8651–8667.

Kornberg MD, Sen N, Hara MR, Juluri KR, Nguyen JV, Snowman AM, Law L, Hester LD, Snyder SH. 2010. GAPDH mediates nitrosylation of nuclear proteins. Nat Cell Biol 12:1094–1100.

Lefebvre P, Benomar Y, Staels B. 2010. Retinoid X receptors: Common heterodimerization partners with distinct functions. Trends Endocrinol Metab 21:676–683.

Lock LT, Tzanakakis ES. 2009. Expansion and differentiation of human embryonic stem cells to endoderm progeny in a microcarrier stirred-suspension culture. Tissue Eng Part A 15:2051–2063.

Maira M, Martens C, Batsche E, Gauthier Y, Drouin J. 2003. Dimer-specific potentiation of NGFI-B (Nur77) transcriptional activity by the protein kinase A pathway and AF-1-dependent coactivator recruitment. Mol Cell Biol 23:763–776.

Maira M, Martens C, Philips A, Drouin J. 1999. Heterodimerization between members of the Nur subfamily of orphan nuclear receptors as a novel mechanism for gene activation. Mol Cell Biol 19:7549–7557.

Morriss-Kay GM, Sokolova N. 1996. Embryonic development and pattern formation. FASEB J 10:961–968.

Myers JM, Martins GG, Ostrowski J, Stachowiak MK. 2003. Nuclear trafficking of FGFR1: A role for the transmembrane domain. J Cell Biochem 88: 1273–1291.

Peng H, Moffett J, Myers J, Fang X, Stachowiak EK, Maher P, Kratz E, Hines J, Fluharty SJ, Mizukoshi E, Bloom DC, Stachowiak MK. 2001. Novel nuclear signaling pathway mediates activation of fibroblast growth factor-2 gene by type 1 and type 2 angiotensin II receptors. Mol Biol Cell 12:449–462.

Peng H, Myers J, Fang X, Stachowiak EK, Maher PA, Martins GG, Popescu G, Berezney R, Stachowiak MK. 2002. Integrative nuclear FGFR1 signaling (INFS) pathway mediates activation of the tyrosine hydroxylase gene by angiotensin II, depolarization and protein kinase C. J Neurochem 81:506–524.

Perlmann T, Jansson L. 1995. A novel pathway for vitamin A signaling mediated by RXR heterodimerization with NGFI-B and NURR1. Genes Dev 9:769–782.

Pfaffl MW. 2001. A new mathematical model for relative quantification in real-time RT-PCR. Nucleic Acids Res 29:e45.

Philips A, Lesage S, Gingras R, Maira MH, Gauthier Y, Hugo P, Drouin J. 1997. Novel dimeric Nur77 signaling mechanism in endocrine and lymphoid cells. Mol Cell Biol 17:5946–5951.

Qiu J, Huang Y, Chen G, Chen Z, Tweardy DJ, Dong S. 2007. Aberrant chromatin remodeling by retinoic acid receptor alpha fusion proteins assessed at the single-cell level. Mol Biol Cell 18:3941–3951.

Qiu J, Shi G, Jia Y, Li J, Wu M, Dong S, Wong J. 2010. The X-linked mental retardation gene PHF8 is a histone demethylase involved in neuronal differentiation. Cell Res 20:908–918.

Reilly JF, Maher PA. 2001. Importin beta-mediated nuclear import of fibroblast growth factor receptor: Role in cell proliferation. J Cell Biol 152:1307–1312.

Rohwedel J, Guan K, Wobus AM. 1999. Induction of cellular differentiation by retinoic acid in vitro. Cells Tissues Organs 165:190–202.

Saucedo-Cardenas O, Quintana-Hau JD, Le WD, Smidt MP, Cox JJ, De Mayo F, Burbach JP, Conneely OM. 1998. Nurr1 is essential for the induction of the dopaminergic phenotype and the survival of ventral mesencephalic late dopaminergic precursor neurons. Proc Nat Acad Sci USA 95:4013–4018.

Sen N, Hara MR, Kornberg MD, Cascio MB, Bae BI, Shahani N, Thomas B, Dawson TM, Dawson VL, Snyder SH, Sawa A. 2008. Nitric oxide-induced nuclear GAPDH activates p300/CBP and mediates apoptosis. Nat Cell Biol 10:866–873.

Shahhoseini M, Taei A, Mehrjardi NZ, Salekdeh GH, Baharvand H. 2010. Epigenetic analysis of human embryonic carcinoma cells during retinoic acid-induced neural differentiation. Biochem Cell Biol 88:527–538.

Smidt MP, Burbach JP. 2009. Terminal differentiation ofmesodiencephalic dopaminergic neurons: The role of Nurr1 and Pitx3. Adv Exp Med Biol 651:47–57.

Somanathan S, Stachowiak EK, Siegel AJ, Stachowiak MK, Berezney R. 2003. Nuclear matrix bound fibroblast growth factor receptor is associated with splicing factor rich and transcriptionally active nuclear speckles. J Cell Biochem 90:856–869.

Stachowiak EK, Fang X, Myers J, Dunham S, Stachowiak MK. 2003a. cAMP-induced differentiation of human neuronal progenitor cells is mediated by nuclear fibroblast growth factor receptor-1 (FGFR1). J Neurochem 84: 1296–1312.

Stachowiak EK, Maher PA, Tucholski J, Mordechai E, Joy A, Moffett J, Coons S, Stachowiak MK. 1997a. Nuclear accumulation of fibroblast growth factor

receptors in human glial cells–association with cell proliferation. Oncogene 14:2201–2211.

Stachowiak EK, Roy I, Stachowiak MK. 2011a. Triggering neuronogenesis by endogenous brain stem cells with DNA nanoplexes. In: Stachowiak MK, Tzanakakis ES, editors. Stem cells from mechanisms to technologies. E.S.T. New Jersey, London, Singapore, Beijng, Shanghai, Hong Kong, Taipei, Chennai: World Scientific Publishing. pp 333–359.

Stachowiak EK, Roy I, Lee Y-W, Capacchietti M, Aletta JM, Prasad PN, Stachowiak MK. 2009. Targeting novel Integrative Nuclear FGFR1 Signaling by nanoparticle-mediated gene transfer stimulates neurogenesis in adult brain. Integr Biol 1:394–403.

Stachowiak MK, Fang X, Myers JM, Dunham SM, Berezney R, Maher PA, Stachowiak EK. 2003b. Integrative nuclear FGFR1 signaling (INFS) as a part of a universal "feed-forward-and-gate" signaling module that controls cell growth and differentiation. J Cell Biochem 90:662–691.

Stachowiak MK, Maher PA, Joy A, Mordechai E, Stachowiak EK. 1996a. Nuclear accumulation of fibroblast growth factor receptors is regulated by multiple signals in adrenal medullary cells. Mol Biol Cell 7:1299–1317.

Stachowiak MK, Maher PA, Joy A, Mordechai E, Stachowiak EK. 1996b. Nuclear localization of functional FGF receptor 1 in human astrocytes suggests a novel mechanism for growth factor action. Brain Res Mol Brain Res 38:161–165.

Stachowiak MK, Maher PA, Stachowiak EK. 2007. Integrative nuclear signaling in cell development-A role for FGF receptor-1. DNA Cell Biol 26:811–826.

Stachowiak MK, Moffett J, Maher P, Tucholski J, Stachowiak EK. 1997b. Growth factor regulation of cell growth and proliferation in the nervous system. A new intracrine nuclear mechanism. Mol Neurobiol 15:257–283.

Stachowiak MK, Stachowiak EK, Aletta JM, Tzanakakis ES. 2011b. A common integrative nuclear signaling module for stem cell development. In: Stachowiak MK, Tzananakis ES, editors. Stem cells from mechanisms to technologies. E.S.T. New Jersey, London, Singapore, Beijing, Shanghai, Hong Kong, Taipei, Chennai: World Scientific. 87–132.

Sun W, Buzanska L, Domanska-Janik K, Salvi RJ, Stachowiak MK. 2005. Voltage-sensitive and ligand-gated channels in differentiating neural stem-like cells derived from the nonhematopoietic fraction of human umbilical cord blood. Stem Cells 23:931–945.

Watson MA, Milbrandt J. 1990. Expression of the nerve growth factor-regulated NGFI-A and NGFI-B genes in the developing rat. Development 110:173–183.

Wilson TE, Fahrner TJ, Johnston M, Milbrandt J. 1991. Identification of the DNA binding site for NGFI-B by genetic selection in yeast. Science 252: 1296–1300.

Wobus AM, Kaomei G, Shan J, Wellner MC, Rohwedel J, Ji G, Fleischmann B, Katus HA, Hescheler J, Franz WM. 1997. Retinoic acid accelerates embryonic stem cell-derived cardiac differentiation and enhances development of ventricular cardiomyocytes. J Mol Cell Cardiol 29:1525–1539.

Woronicz JD, Calnan B, Ngo V, Winoto A. 1994. Requirement for the orphan steroid receptor Nur77 in apoptosis of T-cell hybridomas. Nature 367:277–281.

Zetterstrom RH, Solomin L, Jansson L, Hoffer BJ, Olson L, Perlmann T. 1997. Dopamine neuron agenesis in Nurr1-deficient mice. Science 276:248–250.

Zhang Z, Yoo R, Wells M, Beebe TP Jr, Biran R, Tresco P. 2005. Neurite outgrowth on well-characterized surfaces: Preparation and characterization of chemically and spatially controlled fibronectin and RGD substrates with good bioactivity. Biomaterials 26:47–61.